

HIRDLS

High Resolution Dynamics Limb Sounder

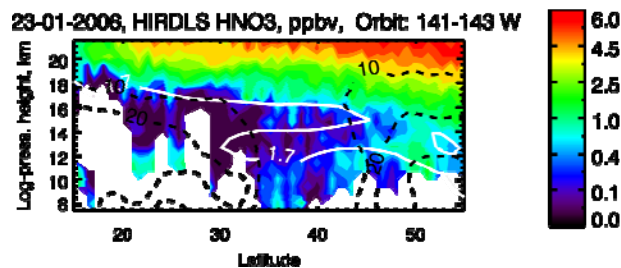
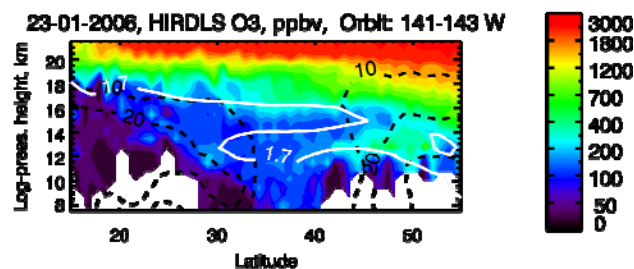
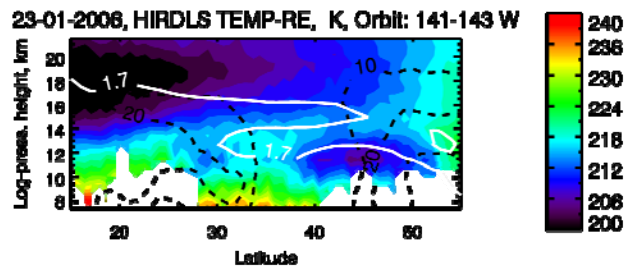
Earth Observing System (EOS)

Data Description and Quality

Version 004

(HIRDLS Version 2.04.19)

September 2008



Oxford University
Department of Atmospheric
Oceanic & Planetary Physics
Oxford, UK

University of Colorado
Center for Limb
Atmospheric Sounding
Boulder, Colorado, USA

National Center for
Atmospheric Research
Boulder, Colorado
USA

Cover Page:

Top Panel: Temperature; showing a double tropopause between 38° - 48° N.

Center Panel: Ozone; mixing ratio, showing a thin layer of air with low ozone extending poleward from the UT into the LS near 14 Km altitude. Its extension follows a region of low scaled potential vorticity (Ertel PV scaled by potential temperature).

Bottom Panel: Nitric acid; mixing ratio, also showing thin layer of UT air with low nitric acid extending into the LS near 14 Km altitude. It also follows the region of low PV.

Acknowledgement:

This research was carried out at the University of Colorado, Boulder and the National Center for Atmospheric Research under a contract (NAS5-97046) with the National Aeronautics and Space Administration.

Table of Contents

1.0 Introduction.....	4
2.0 The HIRDLS Experiment.....	4
2.1 The Experiment as Designed.....	4
2.2 The Launch-induced Anomaly.....	5
2.2.1 History and Present Status.....	5
2.2.2 Impact of Loss of Azimuth Scan Capability.....	6
3.0 Revised Operational Scan Patterns.....	9
4.0 Method for Processing HIRDLS Data.....	9
4.1 L0-1 Process (L1PP, L1X, L1C).....	10
4.2 L2 Pre-processor (L2PP).....	10
4.3 L2 Cloud Detection (L2CLD).....	10
4.4 L1-2 Processor (L2).....	11
5.0 HIRDLS Standard Products.....	11
5.1 Temperature.....	11
5.2 Ozone (O ₃).....	16
5.3 Nitric Acid (HNO ₃).....	25
5.4 CFC11, CFC12.....	35
5.5 H ₂ O.....	43
5.6 CH ₄	43
5.7 NO ₂	43
5.8 N ₂ O ₅	43
5.9 ClONO ₂	43
5.10 Cloud Products.....	44
6.0 Data File Structure and Content.....	51
7.0 Algorithm Changes.....	52
8.0 Acronyms.....	52

1.0 Introduction

As the following sections describe, the entrance aperture of the High Resolution Dynamics Limb Sounder (HIRDLS) was largely obscured by a piece of plastic material that came loose during launch. This resulted in a partial blocking of the signal from the atmosphere, and the addition of extraneous signals from the plastic blockage material. Because of the position of the blockage, coverage of Antarctica and the higher longitudinal resolution expected are precluded, although latitudinal resolution has been increased.

The HIRDLS team has been working since the discovery of this anomaly to understand the nature of the blockage and, to develop four major correction algorithms to make the resulting radiances as close as possible to those originally expected. Corrections for some channels, and therefore the products retrieved from them, have been successful earlier than others, which has led to this current group of retrieved data products. This document provides a description of the second fully-released version of data for the entire mission, which includes retrieved temperature, ozone, nitric acid, chlorofluoro carbons 11 and 12, and aerosol extinction, as well as cloud top pressure.

Work is ongoing to improve the radiances, and the retrievals, for these channels, as well as for those channels whose products are not included in this release.

These data are scientifically important, but it is recognized that they will be improved in future versions. Some of the known problems with the data are described below, but these are almost surely not the only ones. This work is ongoing, and further improvements are being developed and implemented. The HIRDLS team is releasing these data for scientific use and validation, with the expectation that those who look at the data will provide feedback on deficiencies that need to be addressed in future versions, as well as strengths of the data. This document will be updated as additional data products are released, and as other changes dictate.

We strongly suggest that anyone wishing to work with the data contact the HIRDLS team. In the first instance, this should be one of the Principal Investigators (PI's):

John Gille
U.S. P.I.
gille@ucar.edu

John Barnett
U.K. P.I.
j.barnett@physics.ox.ac.uk

2.0 The HIRDLS Experiment

2.1 The Experiment as Designed

HIRDLS is an infrared limb-scanning radiometer designed to sound the upper troposphere, stratosphere, and mesosphere to determine temperature; the mixing ratios of O₃, H₂O, CH₄, N₂O, NO₂, HNO₃, N₂O₅, CFC11, CFC12, ClONO₂, and aerosols; and the locations of polar stratospheric clouds and cloud tops. The goals were to provide sounding observations with horizontal and vertical resolution superior to that previously obtained; to observe the lower

stratosphere with improved sensitivity and accuracy; and to improve understanding of atmospheric processes through data analysis, diagnostics, and use of two- and three-dimensional models.

HIRDLS performs limb scans in the vertical, measuring infrared emissions in 21 channels ranging from 6.12 to 17.76 μm . Four channels measure the emission by CO_2 . Taking advantage of the known mixing ratio of CO_2 , the transmittance is calculated, and the equation of radiative transfer is inverted to determine the vertical distribution of the Planck black body function, from which the temperature is derived as a function of pressure. Once the temperature profile has been established, it is used to determine the Planck function profile for the trace gas channels. The measured radiance and the Planck function profile are then used to determine the transmittance of each trace species and its mixing ratio distribution.

The overall measurement goals of HIRDLS were to observe the global distributions of temperature, the 10 trace species and particulates from the upper troposphere into the mesosphere at high vertical and horizontal resolution. Observations of the lower stratosphere are improved through the use of special narrow and more transparent spectral channels.

2.2 The Launch-induced Anomaly

2.2.1 History and Present Status

HIRDLS was launched on the EOS Aura spacecraft on 15 July 2004. All steps in the initial activation were nominal until the initialization of the scanner on 30 July 2004 indicated more drag than anticipated, and a subsequent health test of the scan mechanism indicated that the damping of the elevation mechanism was $\sim 20\%$ greater than on the ground. After the cooler was turned on and the detectors reached their operating temperature (~ 62 K), initial scans showed radiances much larger and more uniform than atmospheric radiances, except for a region of lower signals at the most negative azimuths. The HIRDLS team immediately identified this as indicating a probable blockage of a large part of the optical aperture.

Tests confirmed that the blockage emits a large, nearly uniform radiance, and covers all of the aperture except a small region 47° from the orbital plane on the side away from the sun.

A number of scan mirror and door maneuvers were conducted in an attempt to dislodge the obstruction, now believed to be a piece of plastic film that was installed to maintain the cleanliness of the optics. None of these maneuvers was successful in improving HIRDLS' view of Earth's atmosphere.

However, these studies and subsequent operations of the instrument have shown that, except for the blockage, HIRDLS is performing extremely well as a stable, accurate and low noise radiometer. These qualities have allowed the HIRDLS team to develop methods for extracting the atmospheric radiance from the unwanted blockage radiance and to retrieve all of the desired species, although not all of them are of sufficient quality to be released at this time. This will allow HIRDLS to meet a significant fraction of the original science objectives.

At this time data are available from 21 January 2005 until 2 January 2008, although occasional days are missing when spacecraft maneuvers took place. In future, the usable portions of these days will be processed. In addition, data from January – March 2008 will eventually be available. HIRDLS stopped acquiring data after 17 March 2008 when the chopper experienced an anomaly. Efforts are now underway to restore it to operation.

2.2.2 Impact of Loss of Azimuth Scan Capability

In its present configuration, HIRDLS can view past the blockage only at the extreme anti-sun edge of the aperture. Vertical scans are made at a single azimuth angle of 47° line of sight (LOS) from the orbital plane, on the side away from the sun. (This differs from the original design, in which HIRDLS would have made vertical scans at several azimuth angles, providing orbit-to-orbit coverage with a spacing of ~ 400 - 500 km in latitude and longitude.) The inability to make vertical scans at a range of azimuths is a definite loss in data gathering, but not a major loss of scientific capability for many of the mission goals. Some of the impacts of the inability to observe at different azimuth angles are:

Changes in coverage

The single-azimuth coverage is plotted in Fig. 2.1, which shows that coverage only extends to 65° S, thus missing all of Antarctica and the S. Polar cap. In the Northern Hemisphere (N.H.) it reaches 82° N. In mid-latitudes, the descending orbit views nearly the same orbit at midnight as the ascending orbit at 3:00pm 9 orbits or 15 hours later.

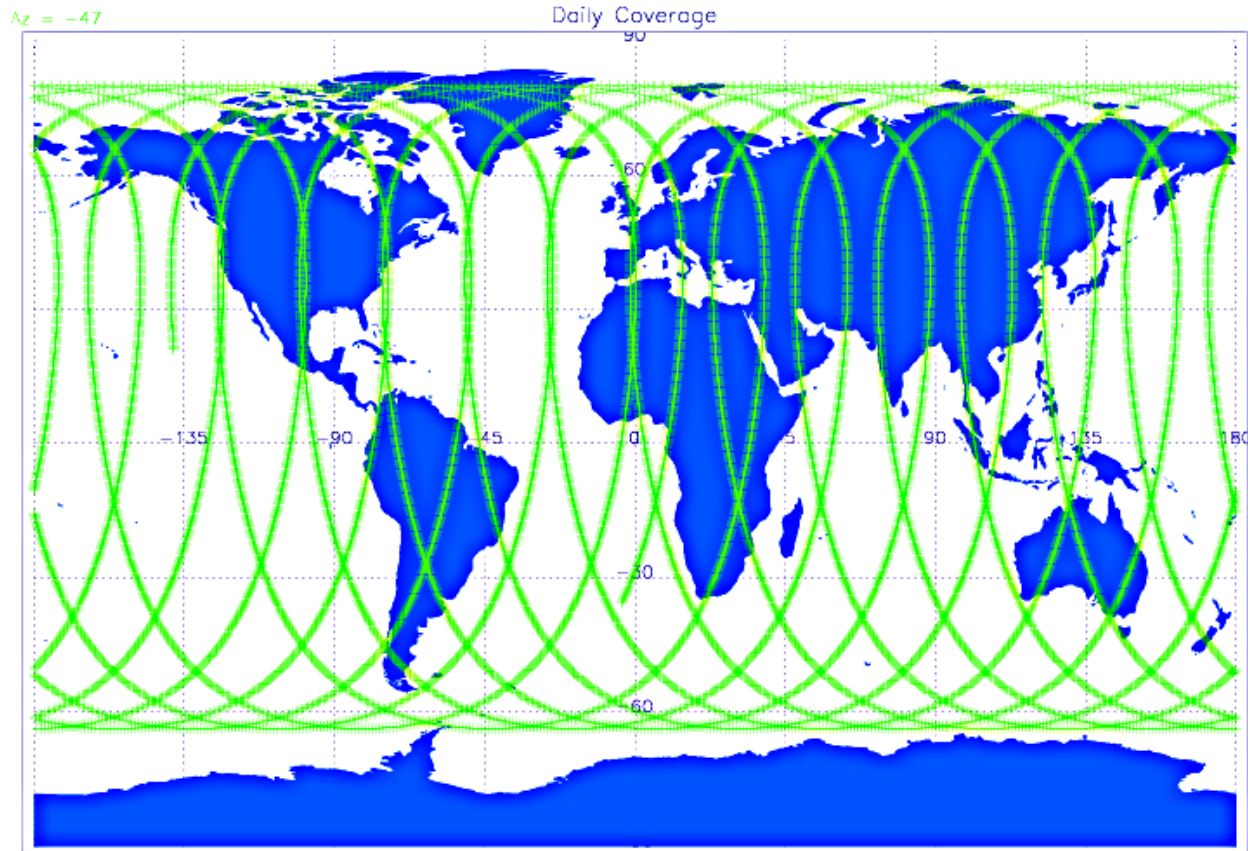


Figure 2.1 HIRDLS Daily Coverage

Inability to View the Same Air Mass as MLS, TES or OMI Within 15 Minutes

The HIRDLS scan track is compared with the MLS scan track in Fig. 2.2. HIRDLS views nearly the same volume as MLS at night (descending part of orbit, left side of figure), but on successive orbits; thus HIRDLS views the same volume 84 minutes earlier than MLS (one orbit, or 99 minutes, minus the 15 minutes that separate MLS views ahead of the S/C and HIRDLS measurements behind the S/C). In the daytime (ascending part of orbit, right side of plot), HIRDLS observations fall 17° to the east of the MLS track in the same orbit, or 8° to the west of the MLS track in the previous orbit. Especially in the daytime, this difference impacts making comparisons, the planning of correlative measurements, and the opportunities to do combined science. However, comparisons and science can easily be done at night where desired.

A corollary feature is that, in the daytime, HIRDLS and MLS combined observe more longitude at a given latitude, which will improve the spatial resolution. At night, together they look at the same volume 84 minutes apart, increasing the temporal resolution.

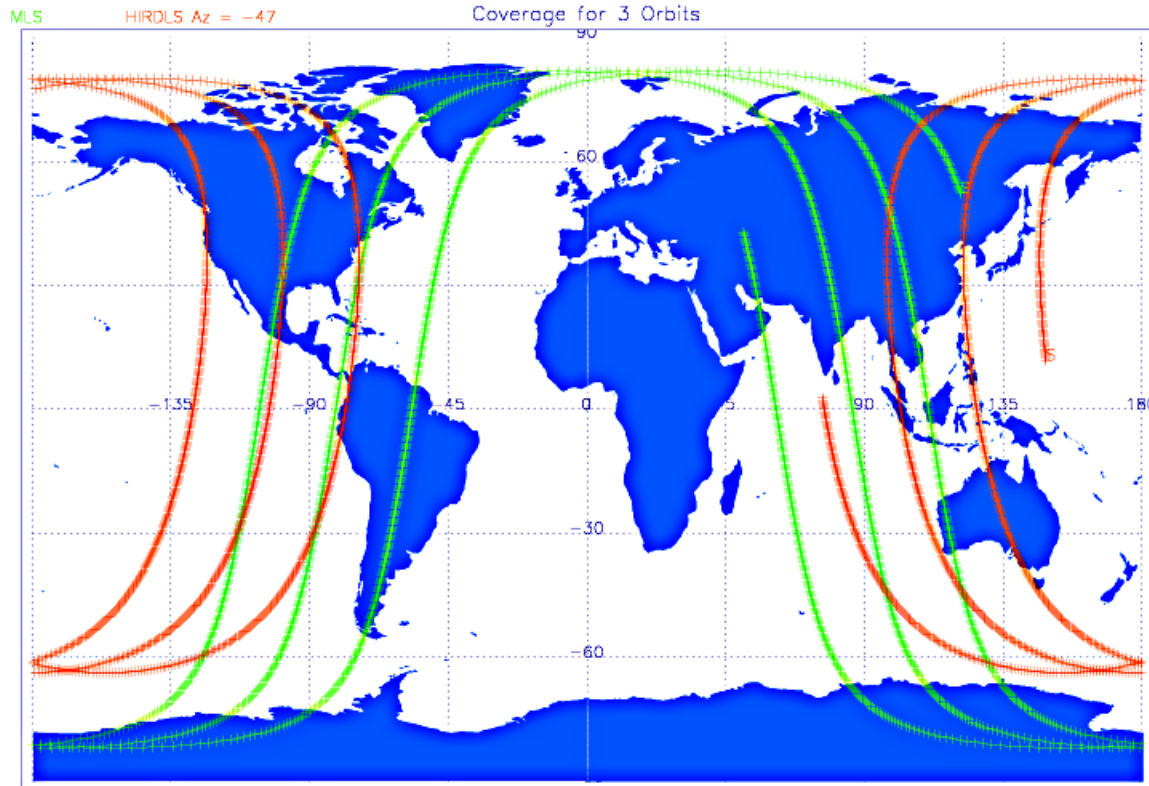


Figure 2.2. Comparison of 3 orbits of HIRDLS (red) measurement locations to MLS (green). HIRDLS is measuring the atmosphere at one azimuth angle (i.e., -47° from the orbit plane). The day and night portion of the orbits are on the right and left side of the figure respectively. During the day part of the orbit, HIRDLS is trailing MLS by one orbit (99-minutes). During the night part of the orbit, the spatial coincidence is much better, although HIRDLS leads MLS by one orbit.

Some compensating effects

With the azimuthal limitation, the profiles will have closer latitudinal separation (~ 100 km), facilitating gravity wave studies. It has also been suggested that transects through tropopause folds might be improved by continuous views at one azimuth.

Since HIRDLS views a long way off the orbital track, as seen above, it measures at a different local time from MLS, TES and OMI. At the northern and southern extremes it means that HIRDLS will get data at a significantly different local time from the other instruments, which could help constrain data assimilation models.

3.0 Revised Operational Scan Patterns

The limited angle at which HIRDLS can see the atmosphere necessitates a revision to previously planned scan patterns. Scans of the atmosphere are done in the region in which the view of the atmosphere is the clearest, at -23.5° azimuth shaft angle, or -47° LOS from the orbital plane (on the side away from the sun).

Science Scan Modes

Scan Table 30 (21 January 2005-28 April 2005). This initial scan used a more rapid vertical scan speed, which generated larger amplitude spurious oscillations in the signals. Because of the difficulty in completely removing these, data from this period are not as good as later data obtained with the other scan tables. This scan also made vertical scans at an LOS azimuth angle of -44.8° , which were found to be inferior to those at -47° .

Scan Table 13: (28 April 2005- 24 April 2006). Upper and lower limits of scans vary around the orbit, following Earth's oblateness. This was discovered to cause different types of oscillations to be seen in the signals, complicating attempts to remove these artifacts.

Scan Table 22: (25 April 2006 to 3 May 2006) Similar to ST 23, but with lower space-ward limit on the scans.

Scan Table 23: (Used since 4 May 2006) It makes slower vertical scans; 27 pairs of vertical up and down scans of ~ 15.5 sec. duration each, followed by a 1-2 second space view before the next 27 scan pairs. To facilitate removal of the oscillations, the space-ward and earth-ward limits of the scans are at fixed elevation scan angles.

4.0 Method for Processing HIRDLS Data

The modified science scans described in Sec. 3 and the need to account for blockage of the scene and radiance from the blockage require substantial modifications to the operational data processing. A diagram of the flow of data in the HIRDLS processing is shown in Figure 4.1.

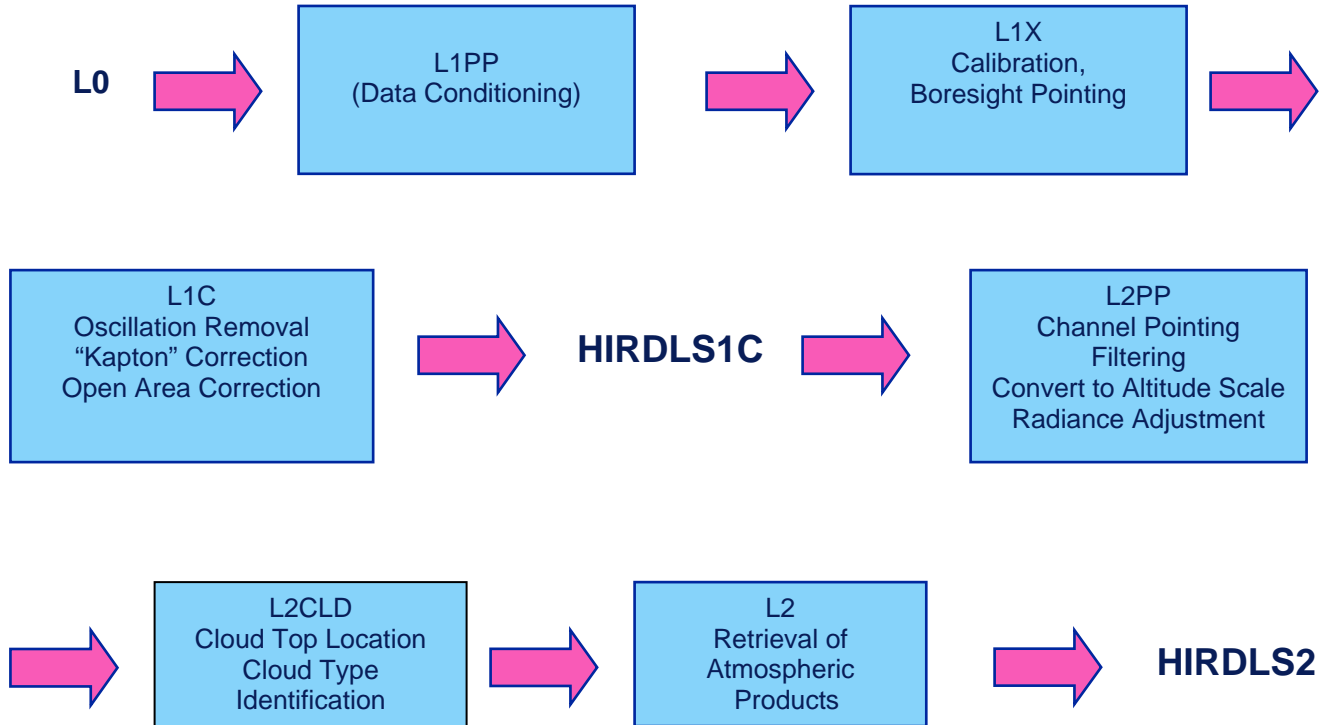


Figure 4.1 HIRDLS Processing Flow

4.1 L0-1 Process (L1PP, L1X, L1C)

In the L0-1 suite of processor, L1PP corrects an occasional problem with the time in L0 data (raw data counts). L1X carries out the modified calibration, and geolocation, while L1C applies the 3 main correction algorithms to remove the effect of the blockage. Overall, the L0-1 processor creates a time series of calibrated radiances blocked into profiles as well as housekeeping data necessary to the further data processing.

4.2 L2 Pre-processor (L2PP)

The L2PP process takes the time series of radiance profiles from L1, separates it into individual geolocated vertical scans, determines the vertical registration in altitude, and performs low-pass filtering to condition the radiances for retrieval by the L1-2 software.

4.3 L2 Cloud Detection (L2CLD)

The L2CLD routine screens for clouds based on detection of radiance perturbations from the average clear sky case. Cloud tops are located and identified.

4.4 L1-2 Processor (L2)

The L2 step accepts the conditioned radiance data from the L2CLD, and performs the retrievals through a series of iterations. This code is designed to be flexible in handling combinations of radiance channels to retrieve the HIRDLS target species in a user-defined sequence. One of the major features is the use of ancillary GMAO data to determine temperature gradients along the line of sight, which are incorporated to yield an improved retrieval. This processor is described in the L1-2 ATBD. GMAO version 5.01 data were used through January 2, 2008, after which version 5.1 data were used.

From December 4-18, 2007, there were problems with the spacecraft data system, resulting in some corrupted data products. Subsequently the input data were reconstructed by the NASA ground data system, and reprocessed in the HIRDLS SIPS. We are not aware of any resulting undetected problems at this time, but users should scrutinize these data carefully.

5.0 HIRDLS Standard Products

5.1 Temperature

Species:	Temperature
Data Field Name	Temperature
Useful Range:	400 – 1hPa
Vertical Resolution	1-2 Km
Contact:	John Gille
Email:	gille@ucar.edu
Validation paper	Gille, J., et al. (2008), High Resolution Dynamics Limb Sounder: Experiment overview, recovery, and validation of initial temperature data, <i>J. Geophys. Res.</i> , 113, D16S43, doi:10.1029/2007JD008824.

Systematic Biases

HIRDLS temperatures have been compared to several data sets in an effort to determine the extent and magnitude of any biases. The results shown here summarize results described by Gille et al. (2008). An important comparison is between radiosondes and nearby HIRDLS temperatures. Fig. 5.1.1 shows comparisons among high resolution radiosonde profiles and 2 nearby HIRDLS retrievals at St. Helena and Gibraltar. The differences in space and time are given. Points to note, in addition to the good agreement, are the way the HIRDLS retrievals follow the small scale vertical structure in the radiosonde data. Note in particular that 1 of the HIRDLS retrievals follows the sharp kink at the lower tropopause exactly, and both follow the double tropopause structure.

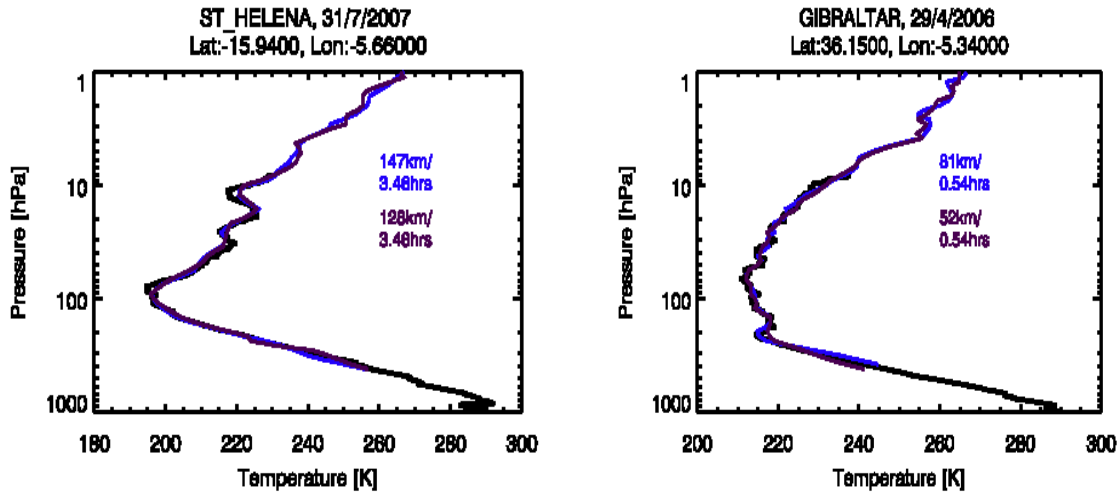


Figure 5.1.1. Temperature comparisons between radiosonde profiles at St. Helena (left) and Gibraltar. Black lines are high resolution radiosondes, blue and magenta are two nearby HIRDLS retrievals. Differences in distances and times are shown.

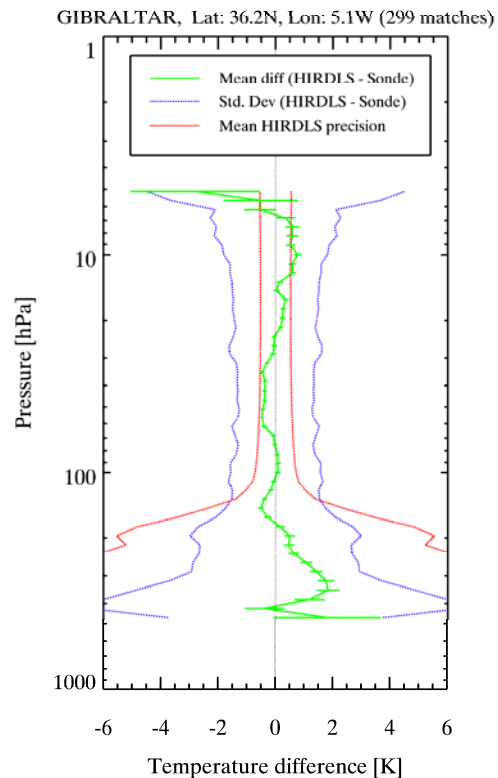


Figure 5.1.2. Statistics of HIRDLS minus sonde differences for Gibraltar. Green line shows mean differences, blue dots show ± 1 standard deviation of the differences, while red dots show ± 1 standard deviation predicted by retrieval algorithm.

Statistics of such comparisons at Gibraltar, a representative site, are shown in Figure 5.1.2. The green line indicates that HIRDLS is within 0.5K of the sondes from ~ 300 hPa to above 10 hPa, with larger differences below 300 hPa. The blue dotted lines are the standard deviation (s.d.) of the differences of HIRDLS minus sondes, while the red dotted lines are \pm the precision value calculated in the retrieval code. Inclusion of the stated precision of the radiosondes does not explain the differences. It is believed that most of the difference comes from differences in time and space between the radiosondes and the HIRDLS profiles, as well as effects of gradients along the HIRDLS line of sight which are not completely corrected. Differences in vertical resolution may also enter. Separate analyses demonstrate that HIRDLS is sensitive to temperature variations with wavelengths as small as 2 km (Gille et al., 2008).

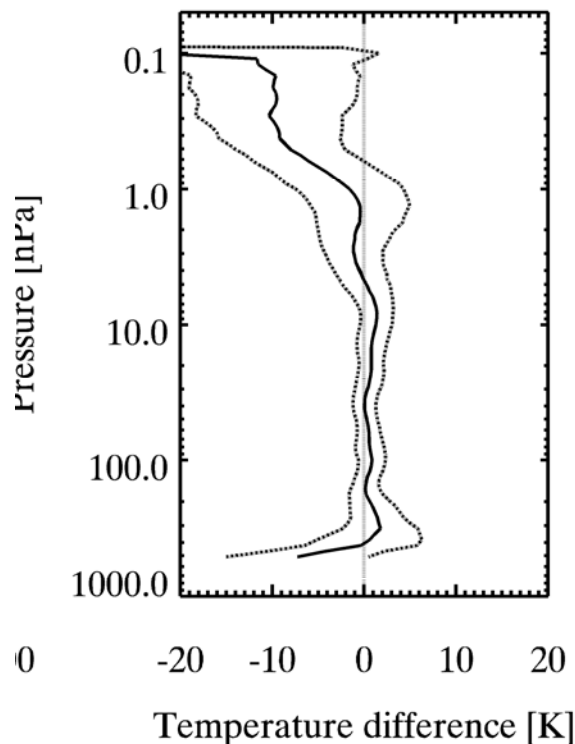


Figure 5.1.3 Results of comparison of HIRDLS temperatures with analyzed ECMWF temperatures interpolated to HIRDLS measurement locations over the full latitude range of HIRDLS observations. The solid line shows HIRDLS minus ECMWF differences ± 1 standard deviation of the differences. Dashed lines indicate ± 1 standard deviation of the differences.

A comparison with the more extensive ECMWF analyses over the HIRDLS latitude range is shown in Figure 5.1.3. From this we see that HIRDLS V004 temperatures are within 1K of ECMWF temperatures from 400 to 1 hPa, becoming lower above that level. This is extremely good, since there are no features seen. The retrieval extends up to 0.1 hPa, with increasing uncertainty above 0.3 hPa. Data at these levels have not been validated, but although there may be biases in the values, the changes seen reflect atmospheric variations..

Temperature precision

One definition of precision is that it is the s.d. of repeated measurements of the same quantity. Following this, one approach to determining the precision of HIRDLS temperatures is to compare repeated views of the same atmosphere, and derive an estimate of the noise from the statistics of their differences. At 80°N and 63°S, successive scan tracks pass over the same points on the Earth's surface one orbit (99 minutes) apart.

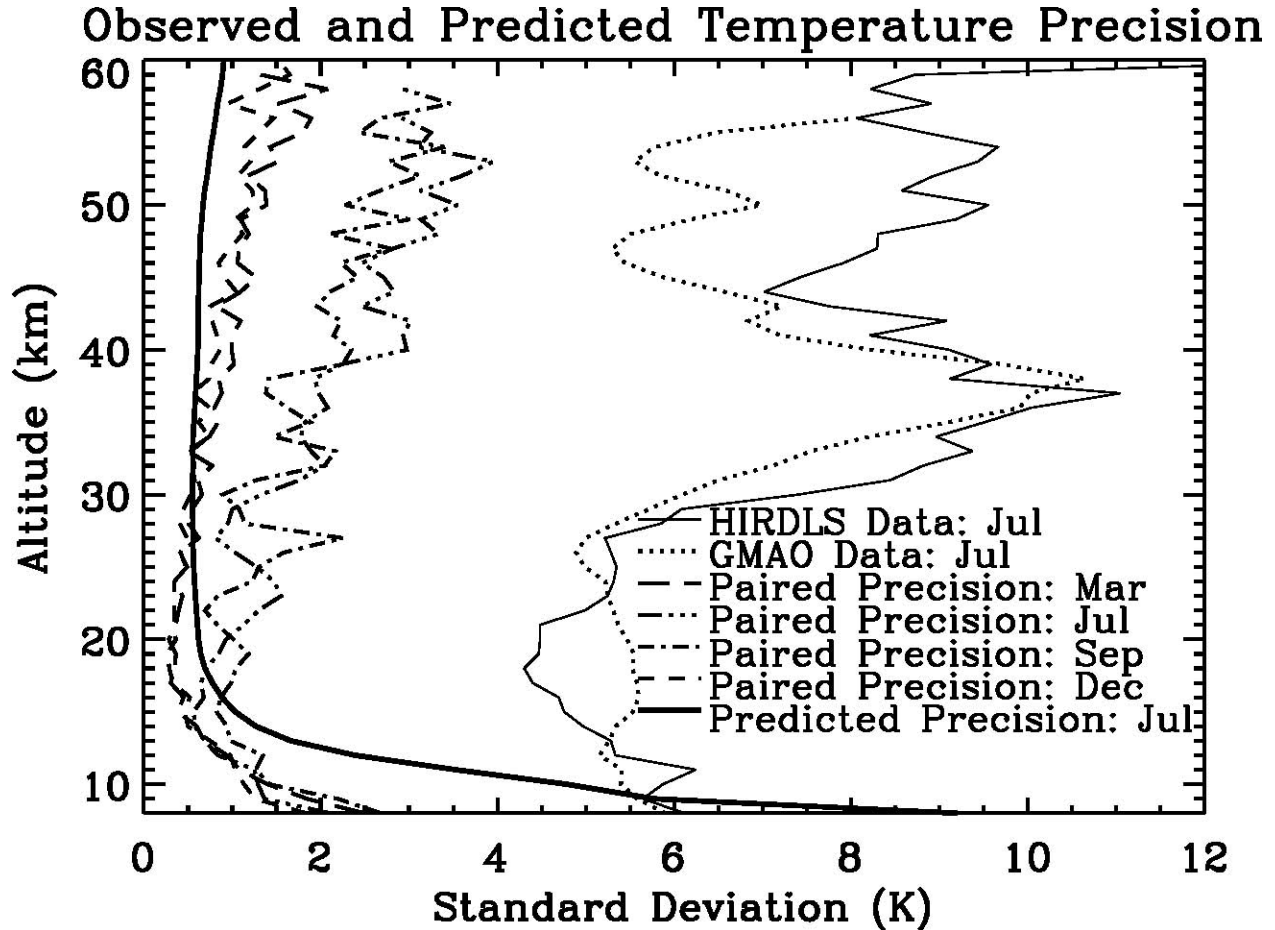


Figure 5.1.4. Empirically determined precision for HIRDLS determined from differences of paired profiles at latitude cross-over points at 63°S for 3 days each in in March, July, September and December, compared to total precision calculated by the retrieval code (solid line). The standard deviations of the GMAO and HIRDLS data for July are also shown. The similarity between the shapes of the December and March curves (summer and fall) and the predicted values gives us confidence that the predicted values are a reasonable indication the true repeatability of HIRDLS temperatures.

Results of this type of analysis are shown in Figure 5.1.4 for 63S for 3 days each season. The pairs of HIRDLS profiles are separated on average by 33 km. The short dashed line shows the precision derived from the differences between the 2 paired HIRDLS profiles after removing the small meteorological changes shown by changes in the GMAO data (RMS value $\leq 0.1\text{K}$ up to 40 km, increasing to 0.8K at 58 km) for December. The thick solid line shows the precision calculated from the parameters in the retrieval code, and shown previously by the dotted red lines in Fig. 5.1.2. The agreement between the predicted and observed precision at the minimum near 20 km, $\sim 0.5\text{ K}$, is reasonably good for this summer season, when a minimum of small-scale dynamical activity is expected. The curves are similar in shape, although the empirical curve increase more rapidly with altitude, presumably because it includes the effects of small-scale motions (e.g. gravity waves) with rapid time scales that have changed in the 99 minute interval between observations. Northern Hemisphere summer values at 80°N (not shown) are very similar. The larger values of the paired precisions, especially at high altitudes during southern winter and spring, when small scale motions should be larger, support this interpretation.

The s.d.'s of GMAO and HIRDLS retrieved temperatures for 3 days in July 2006 are also shown, indicated by the thin solid and dotted lines respectively. The HIRDLS and GMAO variations are similar up to about 40 km, above which the GEOS5 data show larger variations, perhaps reflecting a lack of observational data at those levels. This shows the magnitude of the meteorological variations. These curves show that the noise on the HIRDLS temperatures is much less than the atmospheric variation, making clear that HIRDLS is able to track the meteorological variations to this kind of fidelity.

5.2 Ozone (O₃)

Species	Ozone (O ₃)
Data Field Name:	O3
Useful Range:	1hPa – 260 hPa
Vertical Resolution:	~1 km
Contact:	Bruno Nardi,
Email:	nardi@ucar.edu
Validation Paper:	Nardi, B., et al. (2008), Initial validation of ozone measurements from the High Resolution Dynamics Limb Sounder, <i>J. Geophys. Res.</i> , 113, D16S36, doi:10.1029/2007JD008837.

Differences with V003 [v2.04.09]

The vertical range of useful measurements is extended earthward. The low bias is somewhat diminished, especially in the high latitude lower stratosphere. The much improved cloud detection capability results in far fewer ozone spikes in the UTLS, especially in the tropics. However, the high bias in the tropical UTLS region persists. At low and mid-northern latitudes HIRDLS between 0.3-1 hPa ozone appears within 20% of MLS and MIPAS, but is not validated in this region. Overall the quality of V004 ozone is significantly improved in both vertical range and accuracy.

Accuracy

Comparisons with correlative ozonesonde measurements poleward of about 45 degrees latitude indicate that V004 HIRDLS ozone has an bias of about of 1-10% between 5-200 hPa (figures 5.2.1-5.2.2). Between 200-250 hPa the ozone bias is about 5-20%. Tropical ozonesonde comparisons indicate a 1-10% high bias for p<50 hPa. In the region between 50-100 hPa there is a high bias of ~300 ppbv (~50% at 70 hPa and >150% at 100hPa). It does not appear to be caused by the previously problematic cloud-related ozone spikes, since the improved cloud detection algorithm and post processing filters eliminate these effectively. It may be linked to high variability in ozone in this region which may exceed the relatively low ozone concentrations.

Comparisons with ground-based lidar at Mauna Loa Observatory (20°N) and Table Mountain Facility (39°N) indicate agreement often better than 5% between 1-50 hPa (figure 5.2.3).

Satellite data confirm this general picture. ACE-FTS primarily high latitude satellite solar occultation comparisons (Figure 5.2.4) show a HIRDLS low bias of 5-12% between 2-100 hPa, and up to 20% outside these pressure limits in the Northern Hemisphere [NH] (top, right), and ~2-10% between 0.5-250 hPa in the Southern Hemisphere [SH] (bottom, right).

Ozone differences with MLS on Mercator projection at multiple pressure levels (figure 5.2.5) show agreement within 5% at all latitudes between 3-30 hPa. Agreement is within 10% in the extra-tropics ($|\text{Lat}| > 30^\circ$) between 1-100 hPa. HIRDLS is generally biased low with respect to MLS, except for the previously noted high bias in the tropics (at $p \geq 30$ hPa), and the $\sim 5\%$ high bias in polar regions between 10-30 hPa. The curtain plot comparison with MLS (figure 5.2.6) also shows that HIRDLS generally agrees with MLS to within 10% between 1-100 hPa in the extra-tropics. A slight day / night asymmetry becomes evident, where day-time (ascending node) values tends to be biased slightly high while the night-time values are slightly low. In the extra-tropics between 100-200 hPa HIRDLS agrees with MLS to within 30%, with HIRDLS lower in the NH. In the tropics between 0.2-1 hPa HIRDLS agrees with MLS to within about 20%, with the day/night asymmetry present here.

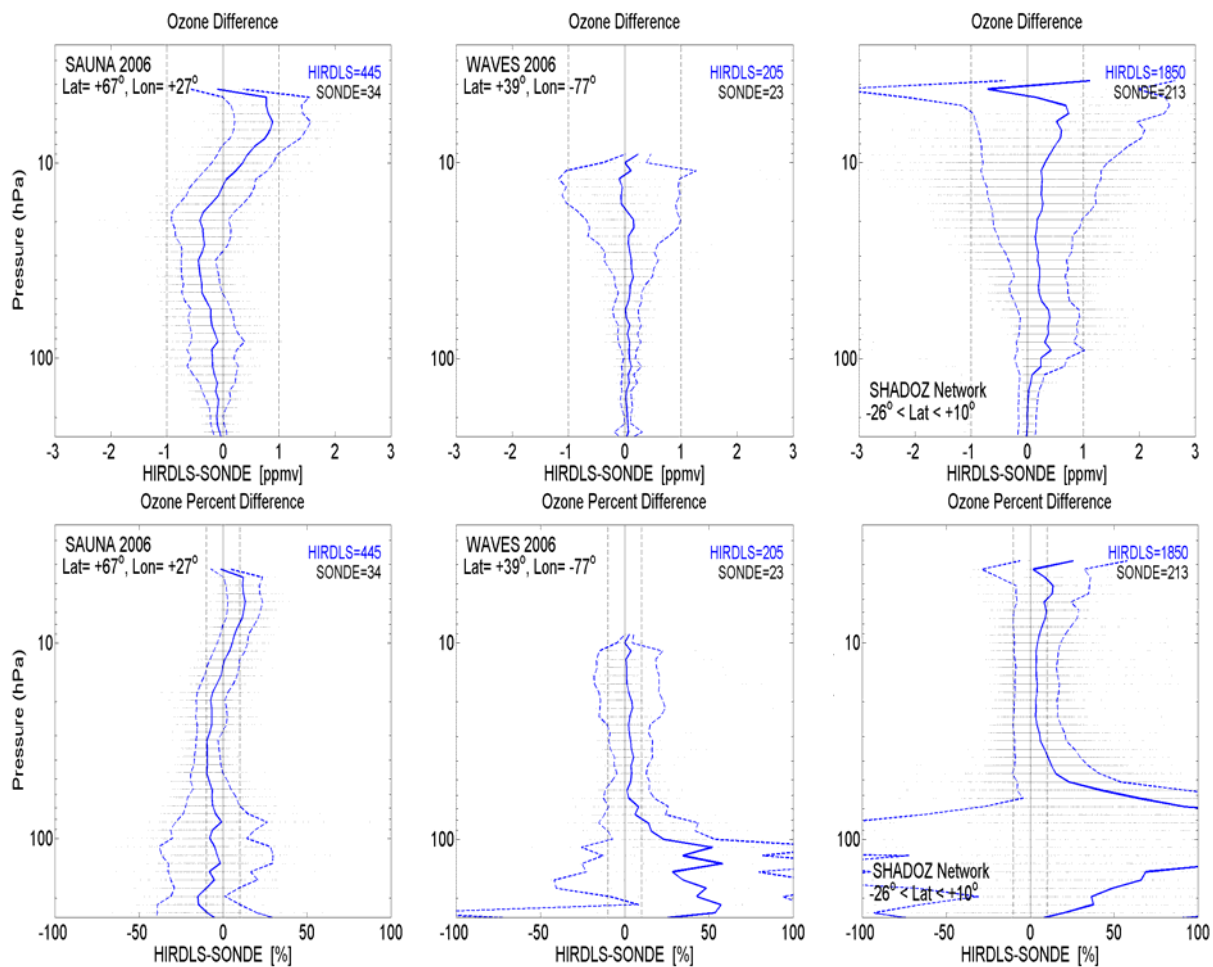


Figure 5.2.1. Shown are the ozone differences in volume mixing ratio [VMR] (top) and percent (bottom) between ozonesondes and HIRDLS coincident profiles for a high latitude campaign, SAUNA (left), a mid-latitude campaign, WAVES (center) and the low latitude SHADOZ network (right). Mean differences (solid blue), standard deviation (dashed blue) and individual differences (black dots) are plotted. Indicated in blue and black in the upper right of each panel is the number of HIRDLS and sonde profiles, respectively, of which the dataset is comprised.

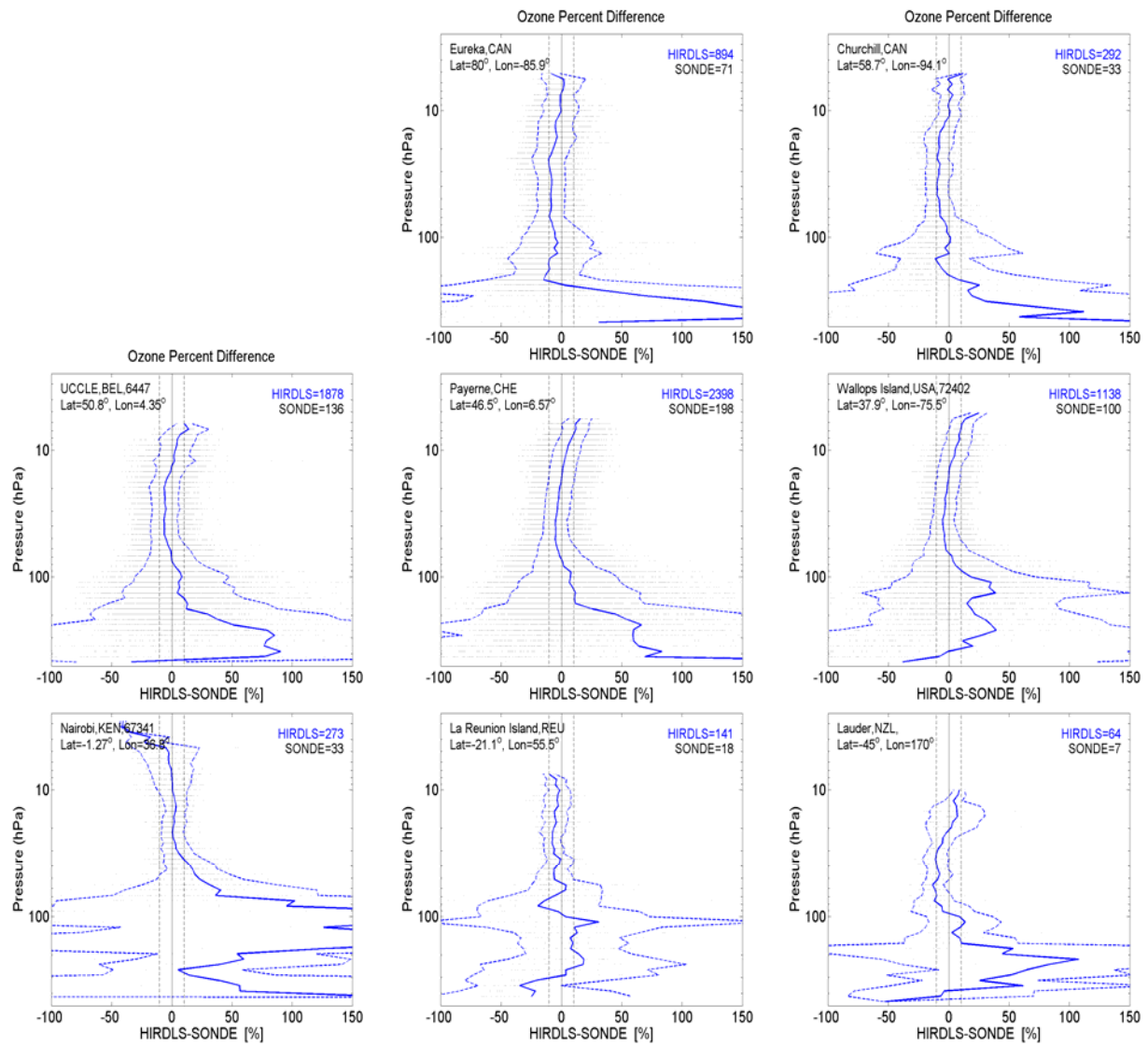


Figure 5.2.2. Shown above are mean ozone difference plots for HIRDLS and ozonesonde for 8 WOUDC (World Ozone and Ultraviolet Radiation Data Center) sites spanning latitude range 45°S to 79°N.

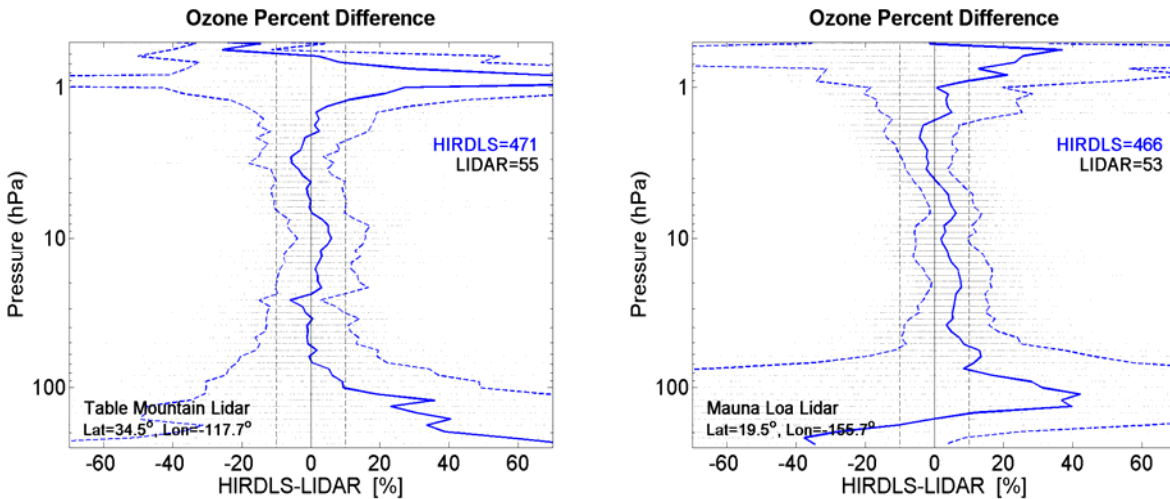


Figure 5.2.3. Shown are the ozone percent differences between 55 TMF lidar profiles and 471 coincident HIRDLS profiles (left), and 53 MLO lidar profiles and 466 coincident HIRDLS profiles (right).

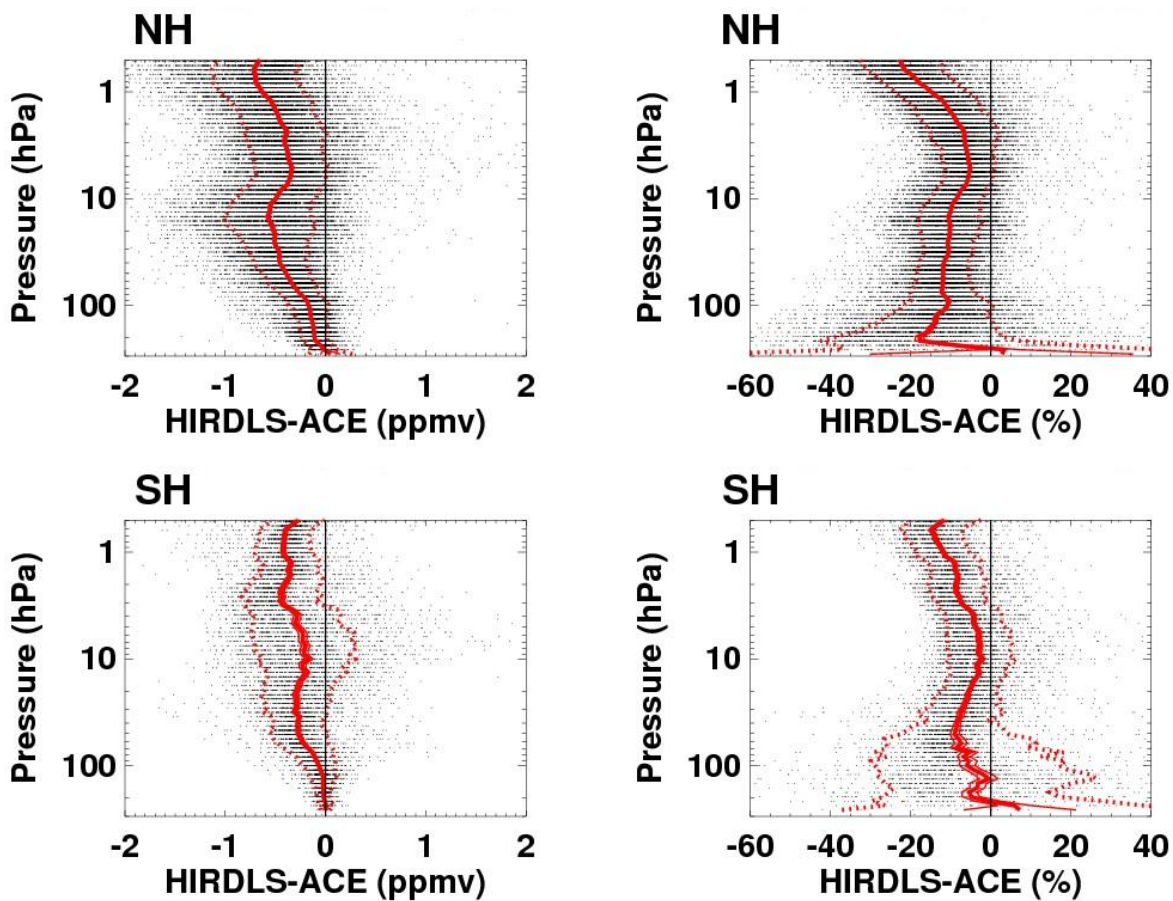


Figure 5.2.4. Shown is the mean and standard deviation of the ozone difference between HIRDLS and ACE-FTS satellite solar occultation measurements (northern hemisphere, top; southern, bottom; VMR, left; percent, right).

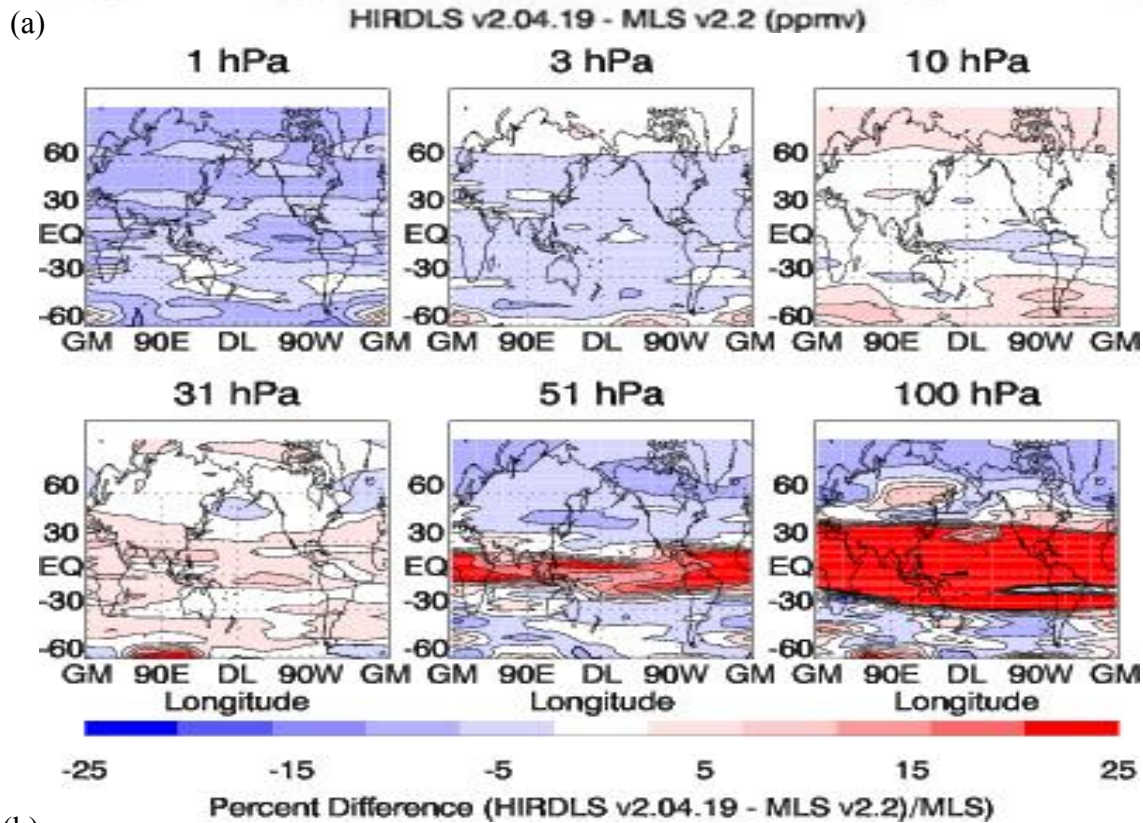
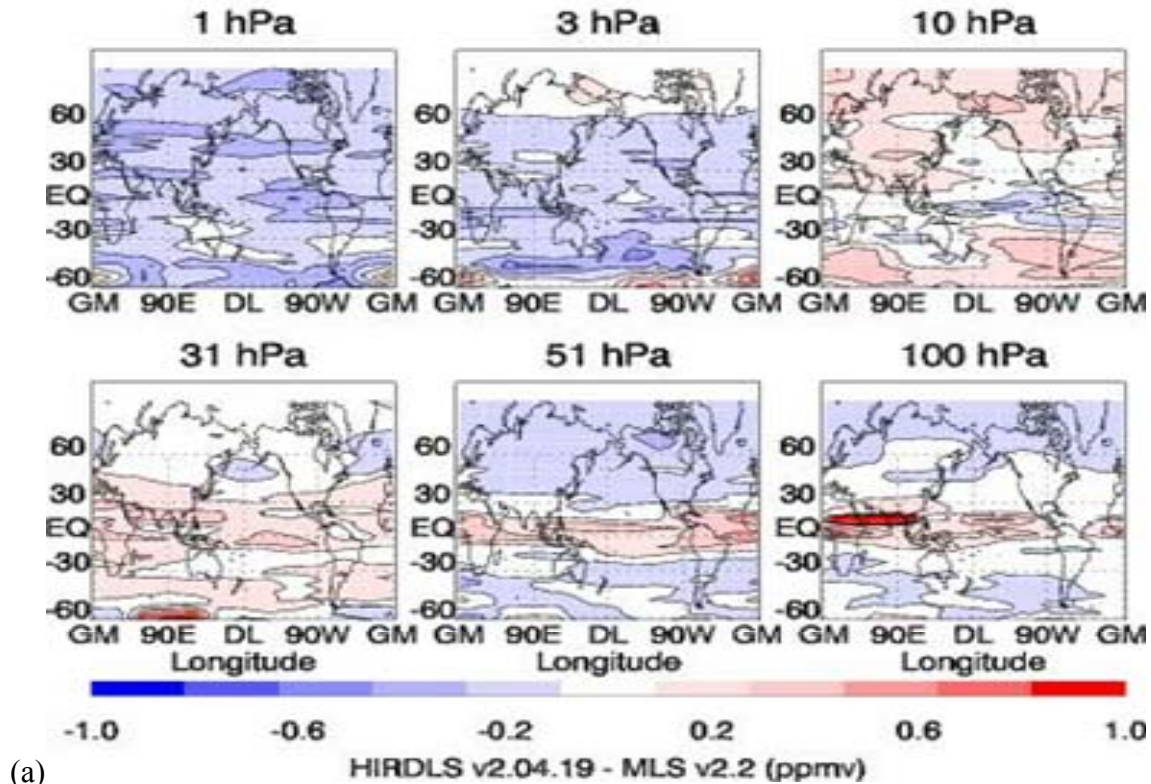


Figure 5.2.5. Mercator representations of the ozone difference in VMR (top) and percent (bottom) between HIRDLS and collocated MLS (v2.2) for 2006-July-15, at pressure levels, 1, 3, 10, 31, 51 and 100 hPa, as indicated over each sub-plot.

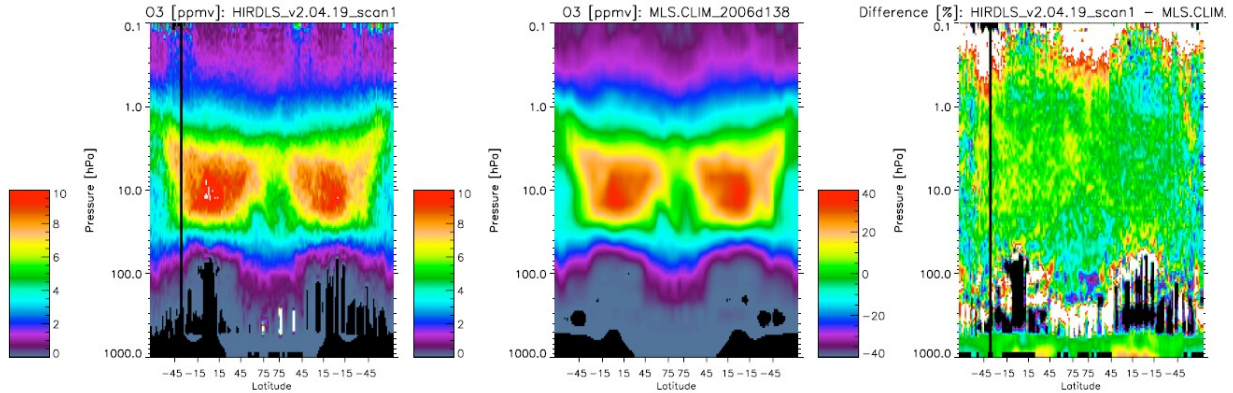


Figure 5.2.6. A single orbit curtain plot comparison with MLS (Left: MLS v2.2; Middle: HIRDLS V004; Right: percent difference). The abscissa indicates the latitude along the track of one orbit. The ascending node of the orbit (day-time) is the left half of each panel while the descending node (night-time) is on the right half.

Precision

The precision is estimated by the standard deviation of ozone binned on an equivalent latitude and potential temperature grid. This is plotted in figure 5.2.7 for June and December 2006. This variability includes both the atmospheric variability and the random error of the HIRDLS data. The atmospheric variability is at a minimum in summer, so the variability shown in summer high latitudes can be taken as an upper bound to the HIRDLS precision. This is estimated to be 5-10% between 1-50 hPa (500-2000K in potential temperature), similar to the case for V003.

High values of the standard deviation at winter-hemisphere high latitudes (LHS of left plot; RHS of right plot) is indicative of the breakdown in these regions, of the effectiveness of binning in equivalent-latitude and potential temperature to remove geophysical variability from the precision estimate, rather than of an actual indication of HIRDLS precision.

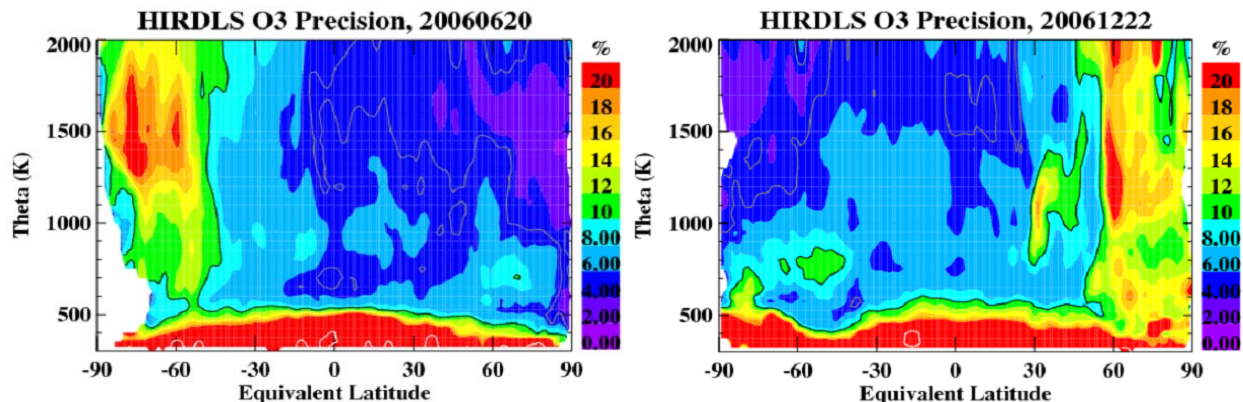


Figure 5.2.7. Shown is the standard deviation of ozone in different equivalent latitude and potential temperature bins, an estimate of HIRDLS ozone precision. Results are given for two days, 2006 June 20 (left) and 2006 December 22 (right), in terms of percentage of ozone mixing ratio.

Vertical Resolution

Comparisons with ozonesondes and lidar give strong indication that HIRDLS is capable of resolving fine vertical ozone features (~ 1 km) in region 1hPa to $>100+$ hPa. Numerous coincident profiles with better than 500 km coincidence show similar layered features. Figure 5.2.8 shows comparisons of HIRDLS ozone with multiple ozonesonde profiles during NH winter/spring when ozone lamina events are prevalent. One can see clearly that the large vertical ozone gradients associated with the ozone lamina are captured very well in the HIRDLS profiles. Comparing over 2600 HIRDLS ozone profiles coincident with about 250 ozonesondes showing strong lamina event, one sees a 0.97 correlation between respective ozone values over all available pressure (figure 5.2.9), giving statistically significant evidence that HIRDLS is able to capture these layers effectively.

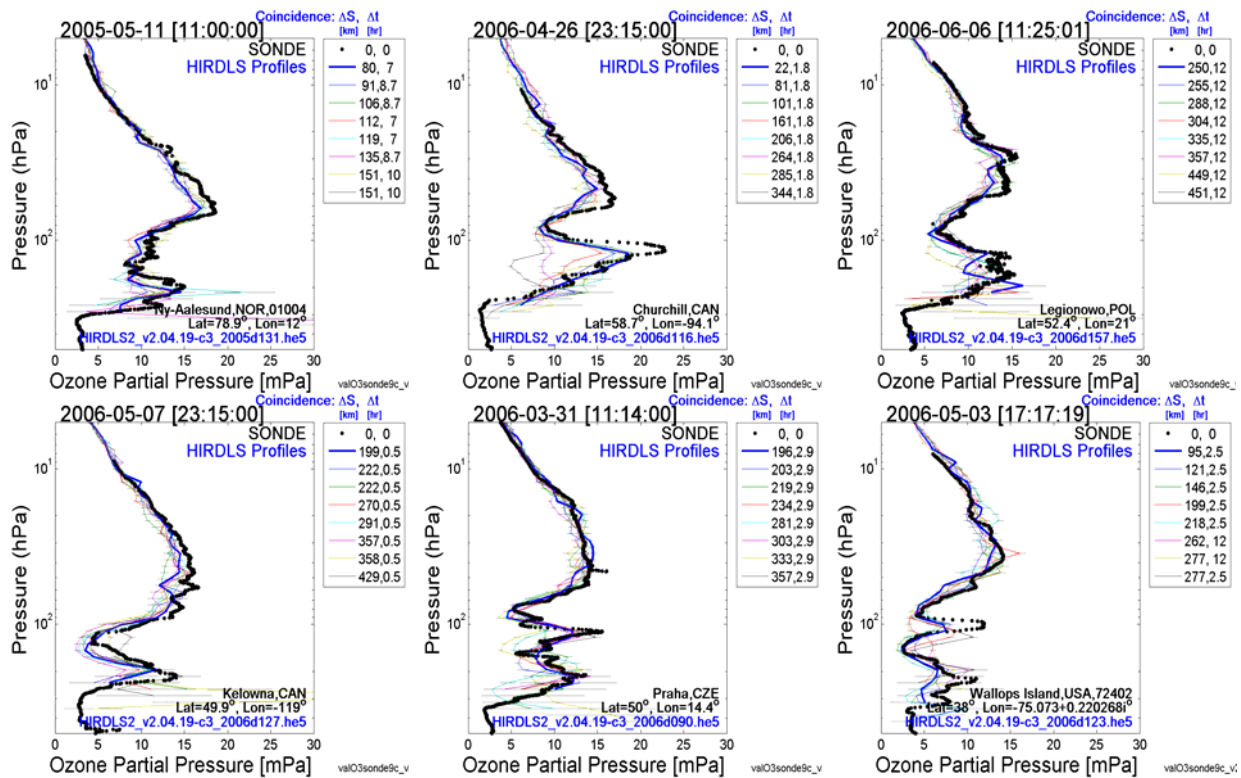


Figure 5.2.8 Comparisons of HIRDLS profiles with multiple ozonesonde profiles. The coincidence criteria used are temporal and spatial separation of less than 500 km and 12 hrs respectively. The black dots are the sonde measurement and the color lines are HIRDLS profiles, the closest coincident profile being in bold-blue.

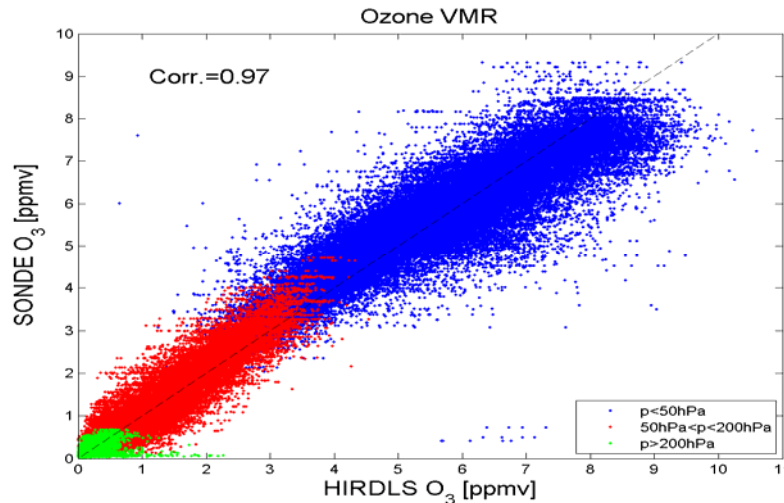


Figure 5.2.9. Shown is a scatter plots of all points from ozone-lamina profiles, in volume mixing ratio. Correlations between the two datasets are very high, at 0.97. The different colors indicate points from different pressure regions, as indicated in the legend. Most laminae are found in the region indicated by red points.

Data Caveats & Artifacts

There is evidence that HIRDLS ozone is useable in the tropics in pressure range, 0.3 - 1 hPa. This is based on comparisons with MLS (Figure 5.2.6) and with MIPAS (not shown) that indicate agreement to within 20%. A full validation in this region has not been conducted however, and data in this region should be used with caution.

The new cloud detection algorithm is much improved over that used in the previous data version (V003). However rare, undetected clouds may be at times be present. These would affect the measured radiance in the ozone channels and results in the large spikes in retrieved ozone. A study of a variety of filters to remove these spikes, and other undesirable ozone data, is summarized below, and a recommendation is given for a relatively effective combination.

Filters for V004 HIRDLS ozone p>60 hPa

Five criteria for filtering ozone earthward of 60 hPa were tested. The criteria are as follows:

1. Negative Precision: Negative values of calculated total retrieval error ("O3Precision") indicate a >50% contribution from a priori to the total error, and thus a strong a priori influence in retrieved ozone;
2. ABS (O3Precision/O3) ratio > 30%: is a more stringent criteria than negative precision;
3. 12.1 MicronCloudAerosolFlag parameter (all points below top-most level where cloud flag $\neq 0$);
4. CloudTopPressure parameter (all points below closest p-level ABOVE indicated pressure);
5. ozone vertical gradient threshold (maximum ozone difference between p-levels)

Figure 5.2.10 shows the HIRDLS ozone, before and after filtering as enumerated above, on multiple pressure levels between 62 - 261 hPa for one 24 hour period on 2006-June-19. Figure 5.2.11 shows a series of staggered profiles for a half orbit during that day. The few spikes observed are removed with filtering.

Evaluation of the results showed that:

1. negative precision filtering is a subset of filtering $ABS(O3Precision/O3) > 30\%$ (ABS=absolute value), and that a ratio of 30% was adequate, decreasing the threshold ratio did not improve spike suppression;
2. 12.1MicronCloudAerosolFlag filtering is a subset of filtering by CloudTopPressure, and that increments (of +1, +2 levels) above CloudTopPressure did not improve spike suppression;
3. filtering on a relatively mild vertical-gradient criteria, >1.9 ppmv/pressure-level (removed) removes all remaining very large spikes.

Based on the observations listed above, the recommended filters for HIRDLS V004 ozone ($p > 60$ hPa) are as follows. All data points should be removed:

- (i) with ratio, $ABS(O3Precision/O3) > 30\%$;
- (ii) at and earthward of the nearest pressure level ABOVE CloudTopPressure;
- (iii) at and earthward of the level where the ozone vertical-gradient criteria threshold of >1.9 ppmv/p-level is reached.

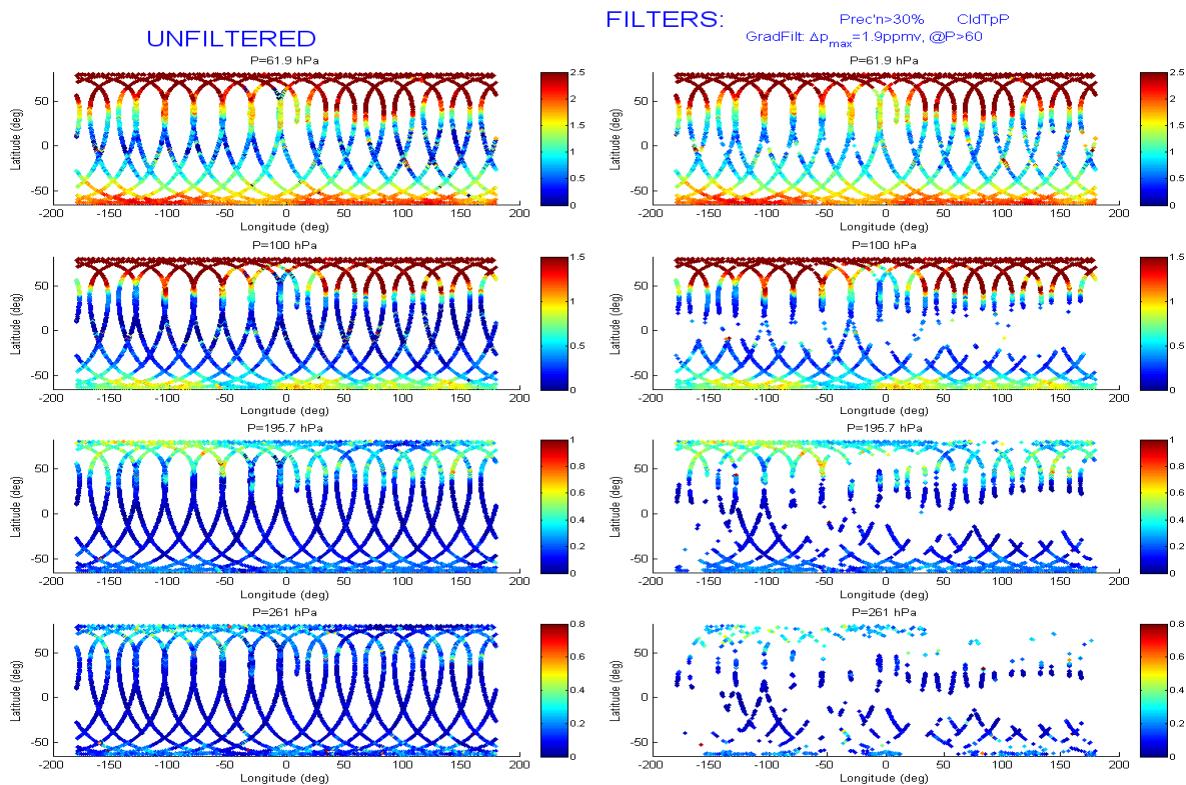


Figure 5.2.10. Shown are HIRDLS V004 ozone on four pressure surfaces (62, 100, 196, 261 hPa) for a 24 hour period on 2006-June-19. At left are the raw unfiltered data and on the right are the filtered data using the three recommended filters.

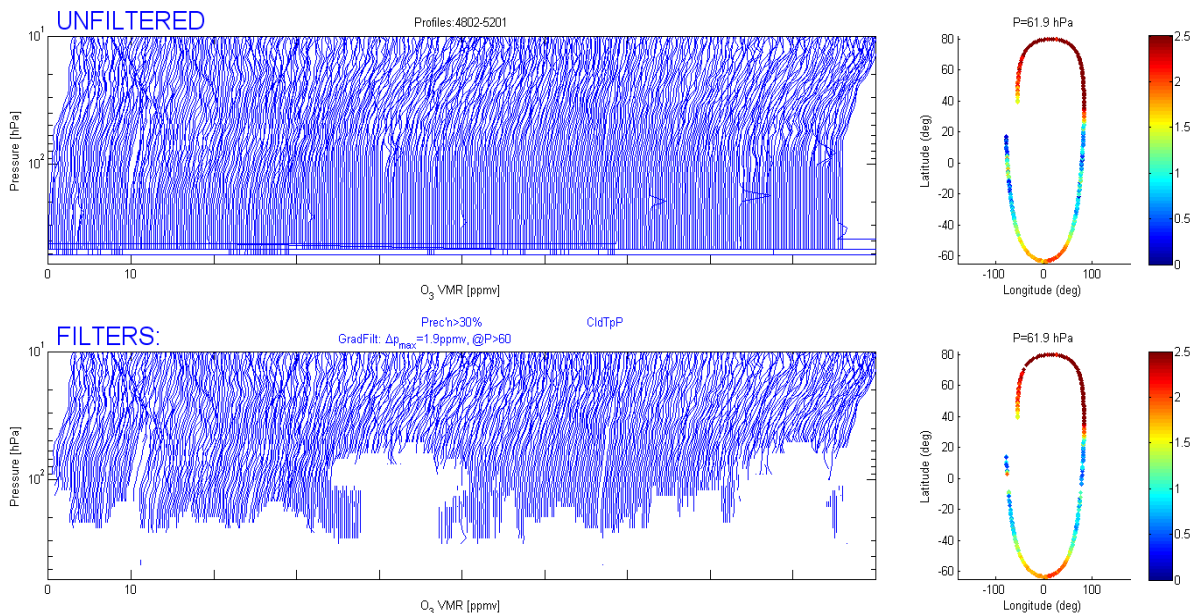


Figure 5.2.11. Shown are HIRDLS V004 ozone profiles for about $\frac{1}{2}$ orbit on 2006-June-19. The top plot shows the raw unfiltered data and the bottom shows the filtered data using the three recommended filters.

5.3 Nitric Acid (HNO₃)

Species:	Nitric Acid (HNO ₃)
Data Field Name:	HNO ₃
Useful Range:	161 hPa – 10 hPa
Vertical Resolution:	~ 1 km
Contact:	Douglas E. Kinnison, NCAR-HIRDLS
Email:	dkin@ucar.edu
Validation Paper	Kinnison <i>et al.</i> , Global observations of HNO ₃ from the High Resolution Dynamics Limb Sounder (HIRDLS) – First results, <i>J. Geophys. Res.</i> , in press 2008.

Early Results and Validation:

HIRDLS HNO₃ data are generally good between 28 April 2005 to the present over the latitude range of 64°S to 80°N and pressure range ~100 hPa to 10 hPa, with some profiles, depending on latitude, having useful information between 100 hPa to 161 hPa. HIRDLS observations before 28 April 2005 (scan table 30) are marginal in quality and not recommended for science applications. The HIRDLS HNO₃ vertical resolution is approximately 1 km, but does vary with altitude and latitude (Figure 5.3.1). The HIRDLS HNO₃ precision was estimated in two ways. The first approach examined the precision as derived by the HIRDLS level-2 retrieval algorithm. We called this the “theoretical” precision. The second approach derived the precision by examining

HIRDLS HNO_3 data in regions of low atmospheric variability. We call this the “measured” precision. The components of the theoretical precision (forward model, measurement, and *a priori* errors) are shown in Figure 5.3.2. This figure shows that for the 100 hPa - 10 hPa (18 - 32 km) region, the contribution of the *a priori* is minimal. However, in the deep tropics, the altitude region where the *a priori* contribution is minimal is smaller (~40 hPa - 10 hPa; ~22 km - 32 km). The HIRDLS HNO_3 at pressures <10 hPa (>32 km) is characterized by large uncertainties and should be used with caution. The individual profile “measured” precision is between 10 - 15%, but can be much larger if the HNO_3 abundance is low or outside the ~100 hPa to 10 hPa range (Figure 5.3.3). Global results are compared with the HNO_3 observations from version 2.2 of the EOS Aura Microwave Limb Sounder (MLS) and it is found that large-scale features are consistent between the two instruments (Figures 5.3.4 and Figures 5.3.5). HIRDLS HNO_3 is biased 0-20% low relative to Aura MLS in the mid-to-high latitudes and biased 50% high in the tropical stratosphere (Figure 5.3.6). More work will be needed to see whether this high bias in the tropics is an issue with the HIRDLS or Aura MLS HNO_3 observations. HIRDLS HNO_3 is also compared with Atmospheric Chemistry Experiment Fourier Transform Spectrometer (ACE-FTS) (Figures 5.3.7 and 5.3.8). In these, high latitude comparisons, the HIRDLS HNO_3 data are biased 10-30% low, depending on altitude.

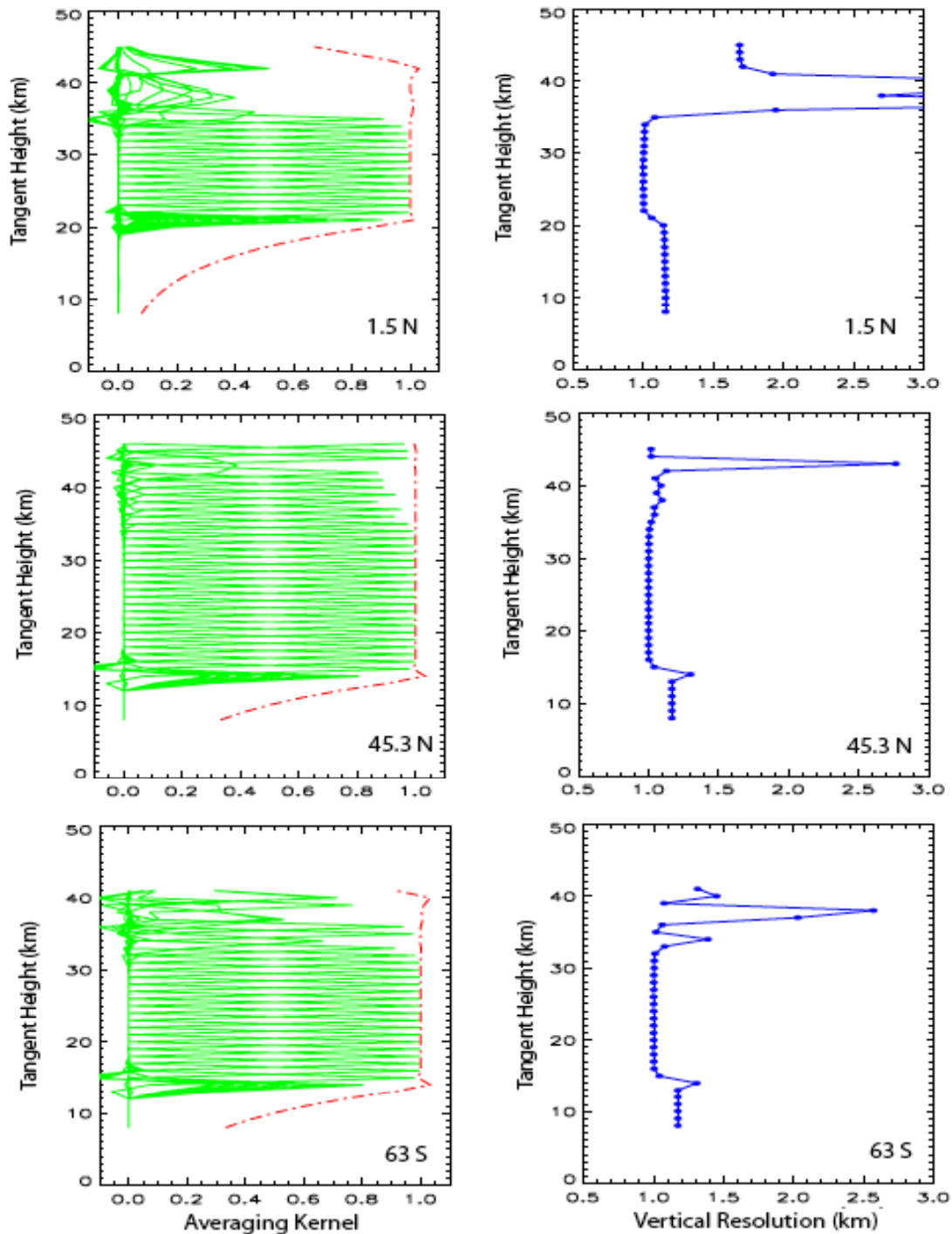


Figure 5.3.1: HIRDLS HNO_3 averaging kernels and full width half maximum (FWHM) vertical resolution profiles are shown on 21 June 2006 at 1.5°N , 45.3°N , and 63°S . The left column shows the averaging kernels (green lines) and the integrated area under each kernel (red line). Where values of unity indicate that all of the information for that vertical region is coming from the measurements and not the *a priori* estimate. The right column represents the vertical resolution as derived from the FWHM of each kernel (blue line).

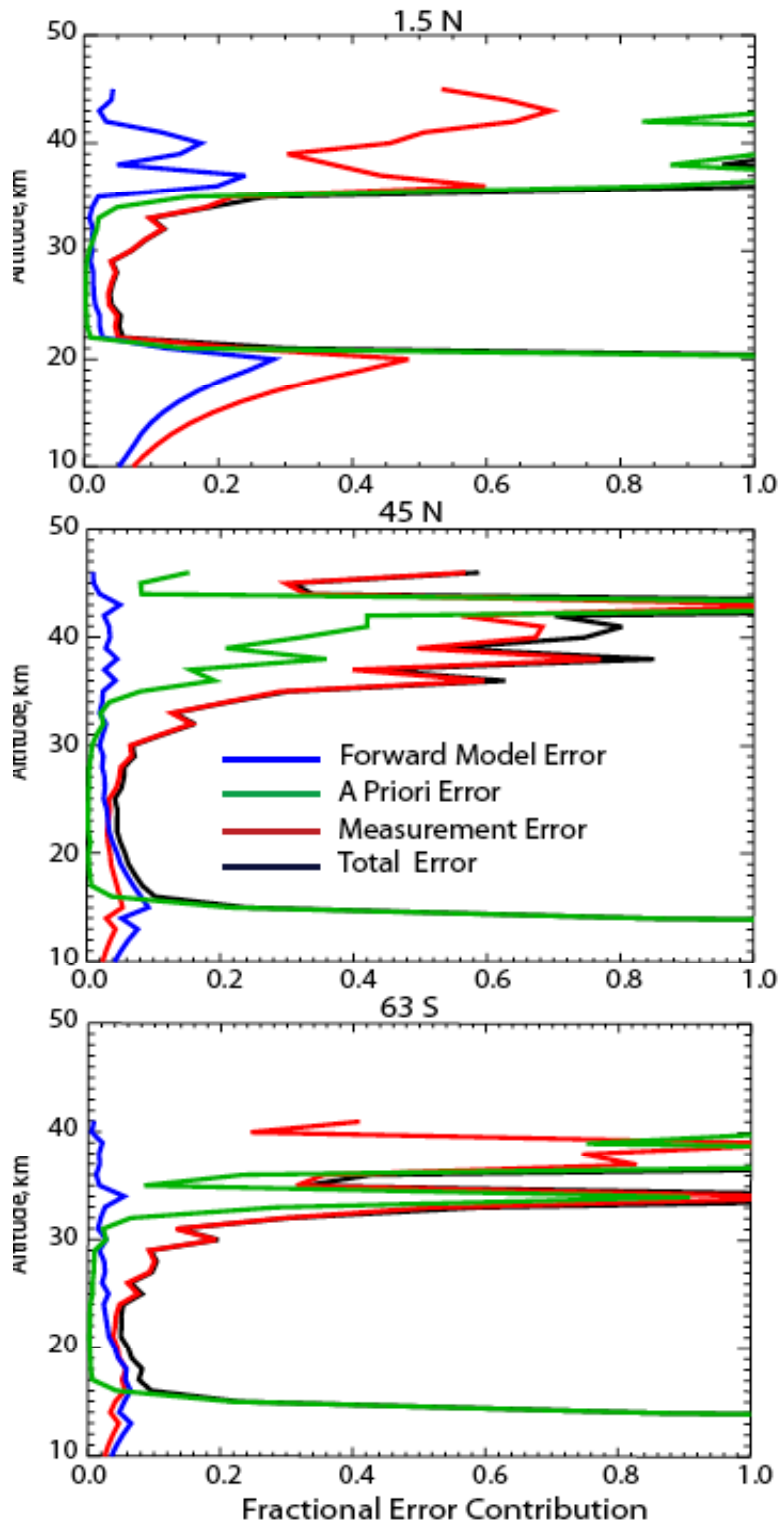


Figure 5.3.2: Shown is the HIRDLs HNO_3 “theoretical precision” displayed as the fractional error contribution for 21 June 2006. The top, middle, and lower panels are for latitudes 1.5°N , 45.3°N and 63°S respectively (same regions as Figure 5.3.1). The forward model error (blue line), the *a priori* error (green line), and the measurement error (red line), along with the total retrieval error (black line) are shown.

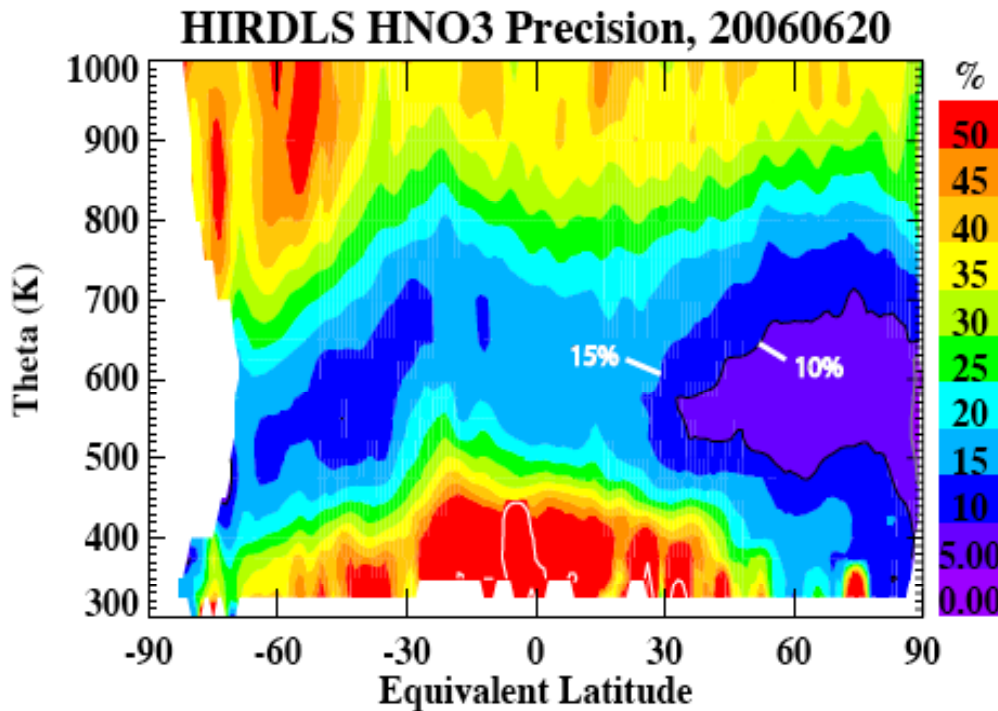


Figure 5.3.3: Shown is the standard deviation of HIRDLS HNO₃ retrievals in a potential temperature and equivalent latitude coordinate system. Results are given for 20 June 2006. Standard deviation units are given in terms of percentage of HNO₃ mixing ratio. The black lines highlight the 10% contour. In this figure we call this estimate of the precision the “measured precision”. To examine the observed variability, 24-hours of HIRDLS HNO₃ were interpolated onto a potential temperature grid and then assembled into 4° equivalent latitude bins centered on 1° increments (essentially 4° wide box-car smoothing in equivalent latitude). The equivalent latitude was derived from Met Office potential vorticity data. In addition, in order to compare air parcels with similar insolation, an additional criterion was imposed. This criterion limits measurements to within 5 degrees of the average geographic latitude in each equivalent latitude bin. The potential temperature range is from 300 to 1000 K or approximately 10 to 35 km. The minimum observed standard deviation is approximately 10 % in this figure. This occurs in the summer hemisphere, where atmospheric variability is known to be a minimum and HNO₃ is abundant (typically >4 ppbv). The theoretical precision (not shown) from the HIRDLS level-2 processor approaches 5% in this region. This figure supports the derivation of the theoretical precision obtained from the level-2 retrieval. Based on this analysis, the theoretical precision may be an underestimate of the true precision, but the error would be on the order of 5% in regions of relatively high abundance of HNO₃.

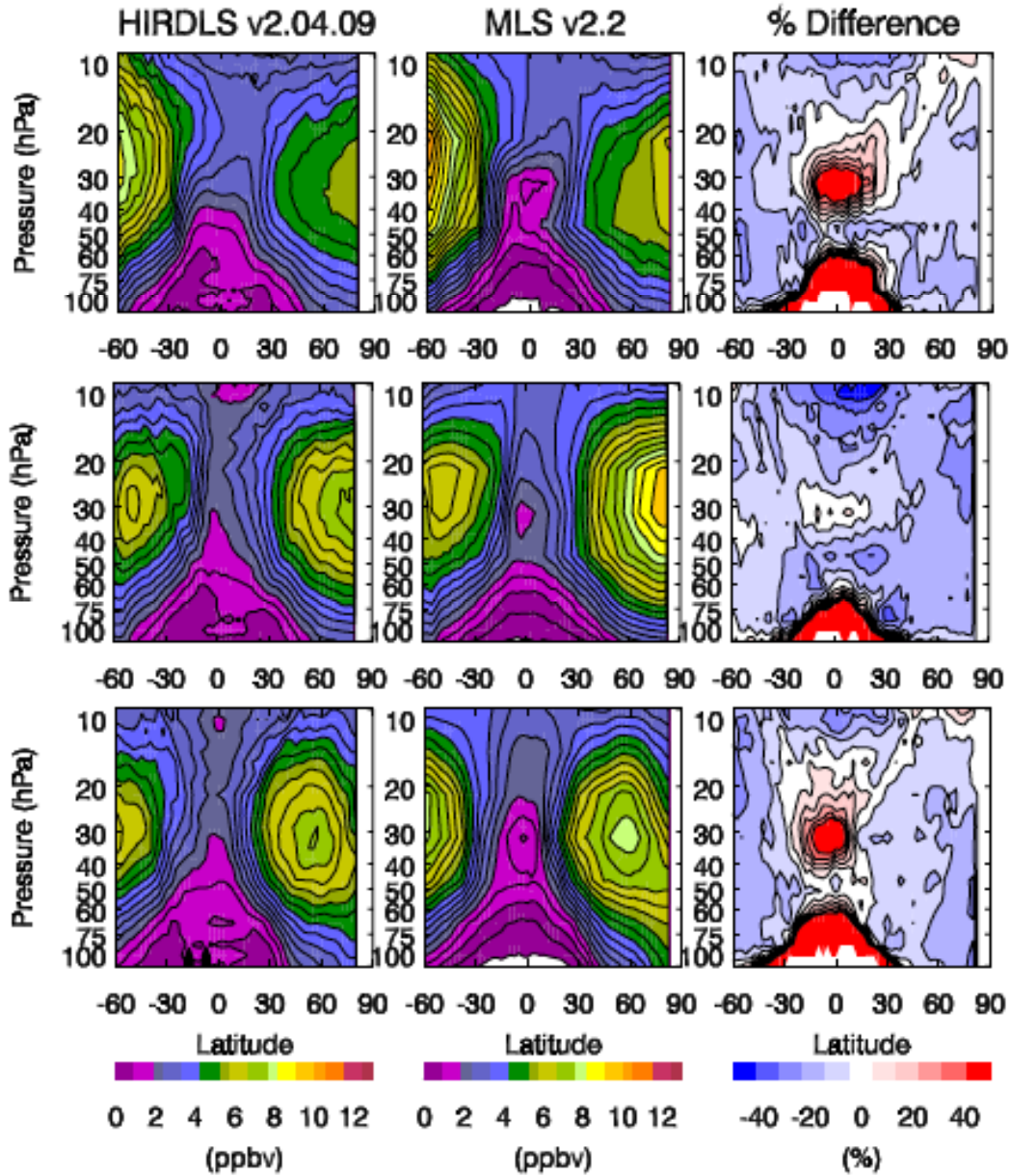


Figure 5.3.4. Latitude-height cross sections are shown for HIRDLS and MLS HNO₃ (ppbv). The top panel is a zonal mean average of four days (in May 2006). The middle panel is a zonal mean average of eight days (in October 2006). The bottom panel is a zonal mean average of 27 days (in March 2007). The percentage difference of $(\text{HIRDLS} - \text{MLS}) / \text{MLS}$ is also shown. The zero percentage difference contour line is the transition from white to blue.

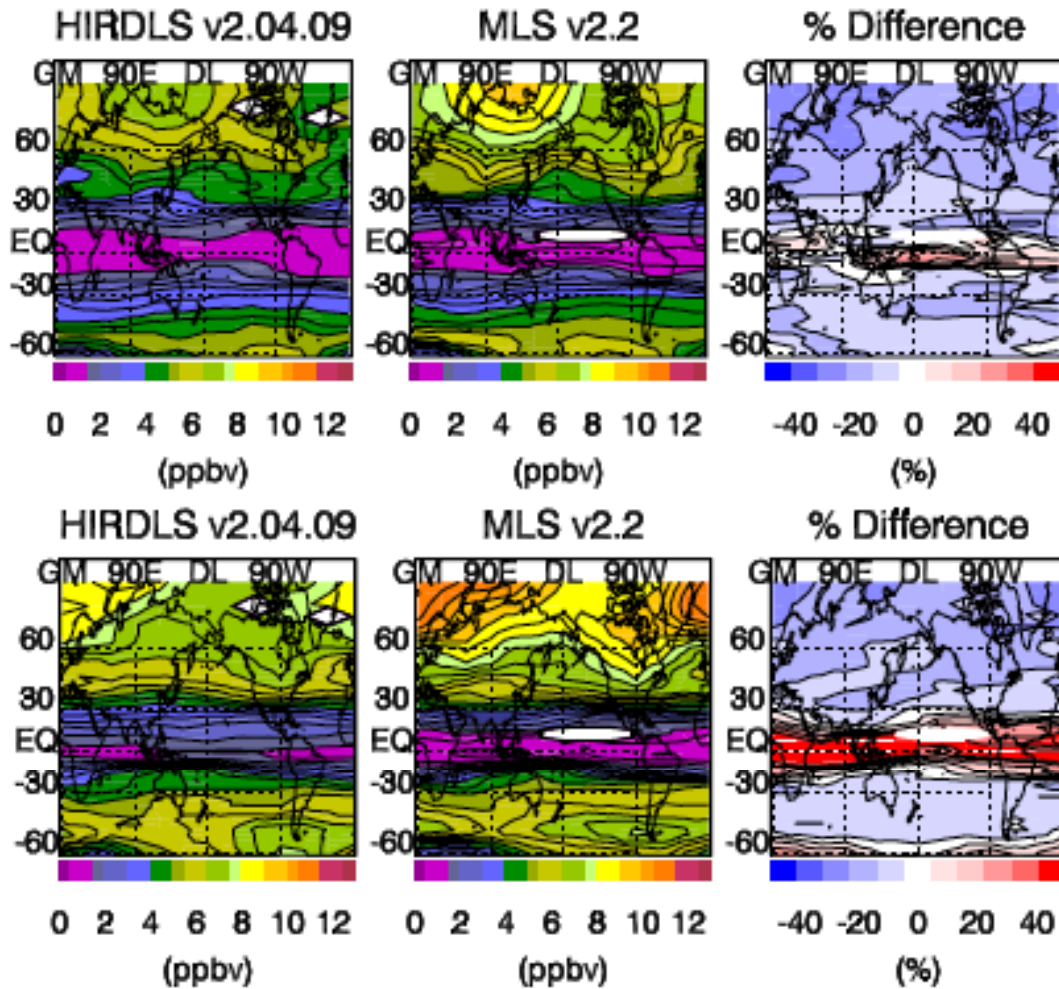


Figure 5.3.5. Longitude-latitude cross sections of HIRDLS and MLS HNO₃ (ppbv) on 28 October 2006. The top and bottom rows are for 51.1 hPa and 31.6 hPa respectively. The percentage difference of $(\text{HIRDLS} - \text{MLS}) / \text{MLS}$ is also shown. The zero percentage difference contour line is the transition from white to blue.

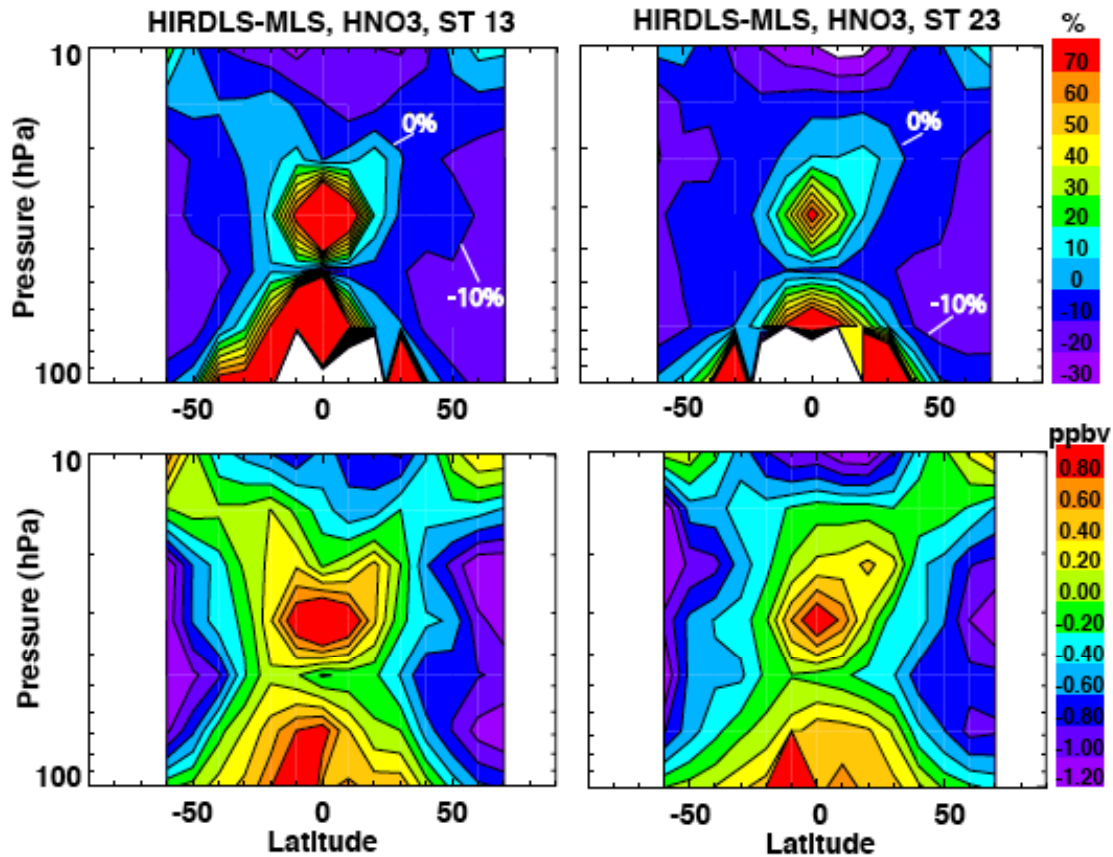


Figure 5.3.6. Latitude-height cross sections of HIRDLS-MLS coincidences for two different HIRDLS scan tables. The left column is for scan table 13; the right column is for scan table 23. There were 165,513 and 67,595 coincidences used to create the panels for scan tables 13 and 23 respectively. The top row shows the percentage difference of $(\text{HIRDLS} - \text{MLS}) / \text{MLS}$. The bottom row shows the absolute differences in volume mixing ratio units (ppbv).

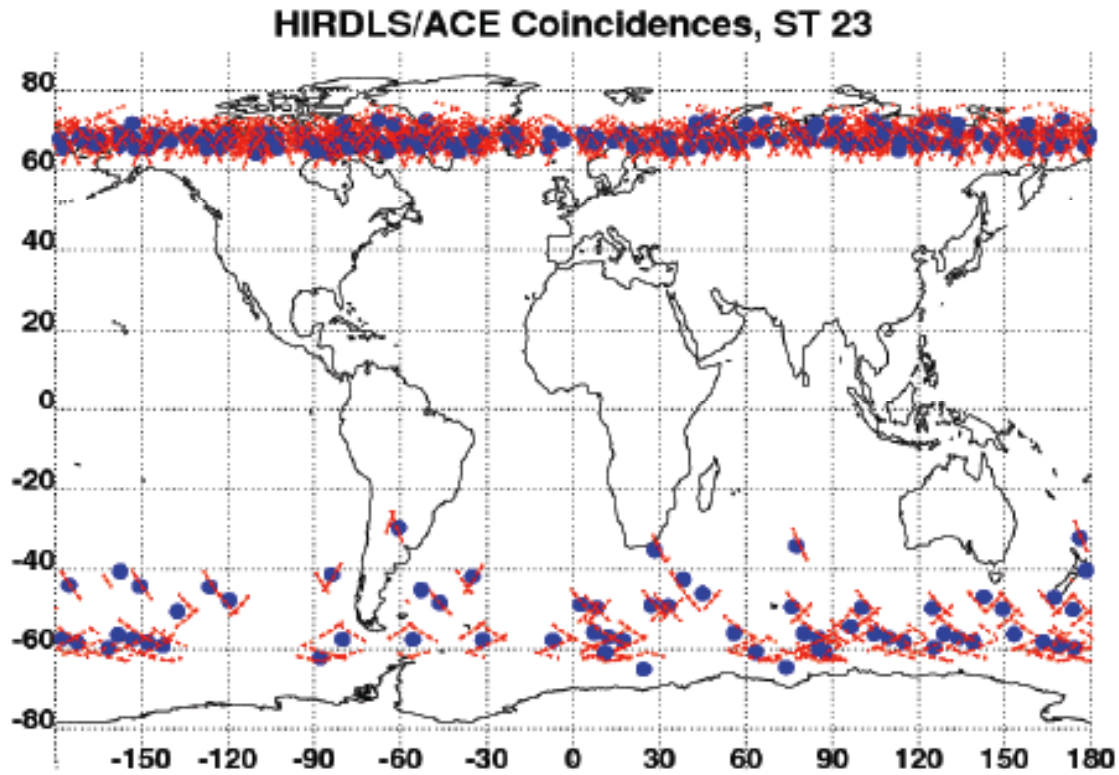


Figure 5.3.7. Latitude-longitude cross sections showing ACE-FTS HNO_3 measurement locations (blue) and HIRDLS HNO_3 measurement locations (red). Coincidences are defined as occurring within 2-hours in time and 500 km. The coincidences shown here are for scan table 23. There were a total of 150 coincidences between 19 May 2006 and 31 October 2006.

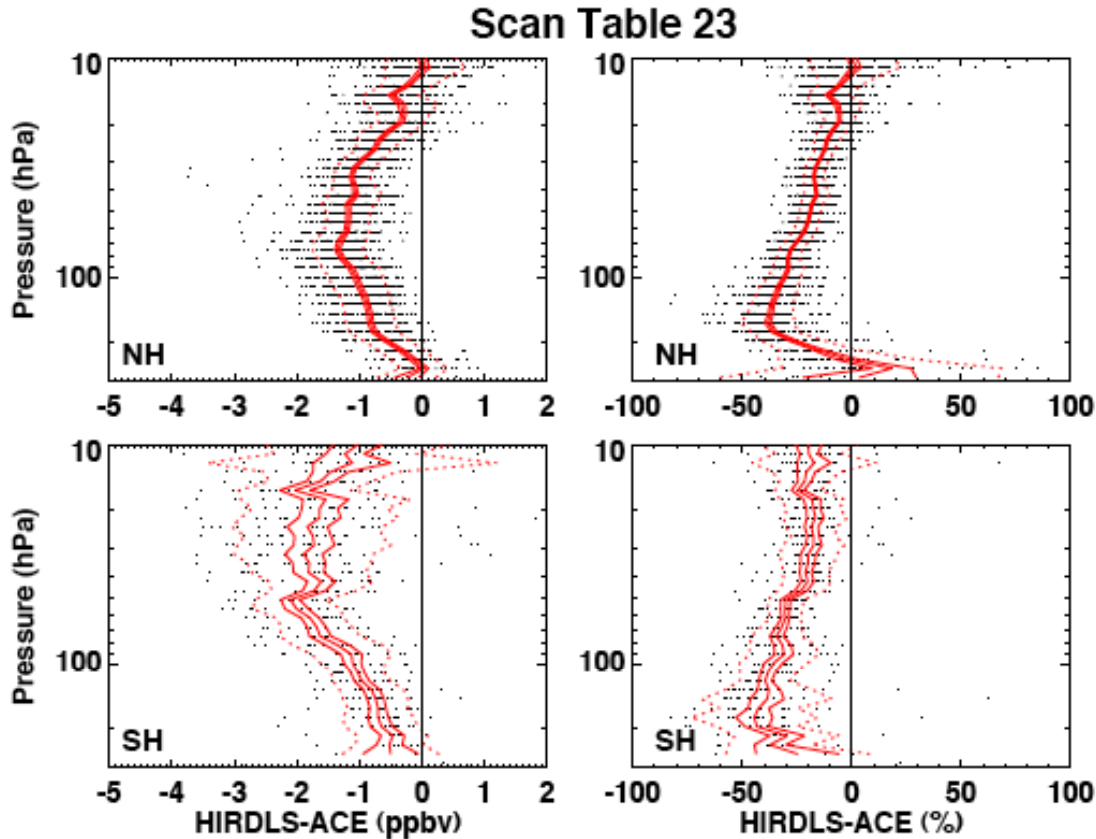


Figure 5.3.8. Profile differences of HIRDLS and ACE-FTS for the scan table 23 measurements. Comparisons shown here were between 19 May 2006 and 31 October 2006 (see Figure 5.3.5). Coincident HIRDLS profiles were averaged together and then subtracted from a single ACE-FTS profile. The top row shows the percentage difference of $(\text{HIRDLS} - \text{ACE-FTS}) / \text{ACE-FTS}$. The bottom row shows absolute differences in volume mixing ratio (ppbv). The mean (solid red) and standard deviation (dashed red) of the differences for all coincidences are shown. The individual differences from which these are derived are the horizontally distributed layers of small black dots. The thin red lines bracketing the mean are the uncertainty in the mean (standard deviation divided by the square root of the number of points).

Acknowledgements: The HIRDLS team would like to thank both the EOS Aura MLS science and the ACE science teams for making their data available for HIRDLS validation.

5.4 CFC11, CFC12

Species:	CFC11 (CFCl ₃) CFC12 (CF ₂ Cl ₂)
Data Field Name:	CFC11 CFC12
Useful Range:	CFC11 26.1 hPa – 287.3 hPa CFC12 10.0 hPa – 287.3 hPa
Screening Criteria:	Use with caution: Data with negative precisions Data with cloud flag $\neq 0$ - data should not be used CFC 11 data above surface value (approx. 250pptv) CFC 12 data above surface value (approx. 540pptv)
Vertical Resolution:	~1 km
Contact:	Michael Coffey
Email:	coffey@ucar.edu

This section will describe HIRDLS observations of CFC11 (CFCl₃) and CFC12 (CF₂Cl₂). These human-made gases have common sources, distributions and chemistry in the atmosphere and will be discussed together here.

HIRDLS Observations

HIRDLS CFC measurements are generally useful between latitudes of 65 S to 82 N and within pressure ranges of 26.1 – 287.3 hPa (about 10 to 25 km) for CFC11 and 10.0 – 287.3 hPa (about 10 to 31 km) for CFC12. Observations should only be used for dates after 28 April 2005 when an appropriate scan pattern was in use by HIRDLS (see section 3.0). Vertical resolution of the CFC observations is described by the vertical averaging kernel and is shown in Figure 5.4.1. There is some variation in the vertical resolution with latitude but that variation is small within the useful pressure range. As may be seen in Figure 5.4.1 the vertical resolution for both CFC11 and CFC12, over the useful pressure range, is 1.0-1.2 km. The horizontal resolution of the observations is approximately 100 km along an orbit track with an orbital separation of about 24 degrees of longitude (about 2000 km at 40N), (see section 2.2.2). Average precision of the zonal mean for CFC11 and CFC12 is about 30% for the useful pressure region. Comparisons are made with other global observations of CFC11 and CFC12. It should be noted that data outside of the useful range has been eliminated from the publicly released data.

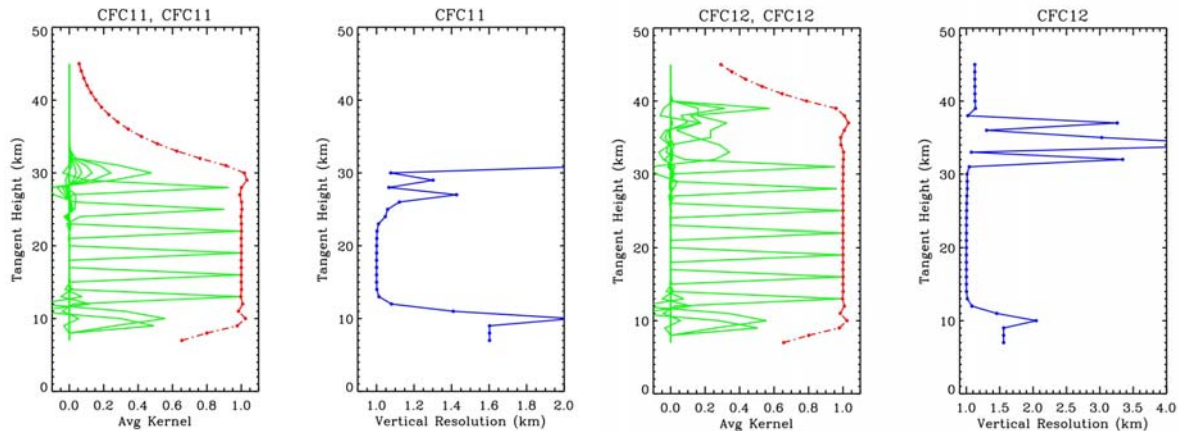


Figure 5.4.1: HIRDLS CFC11 and CFC12 averaging kernels and vertical resolution profiles (full width half maximum, FWHM) for 45.6 N on 15 January 2007. The left column shows averaging kernels (green lines) and the integrated area under each kernel (red line). Values of unity indicate that all of the signal for that vertical region comes from the measurement and not from *a priori* information. The right column shows the vertical resolution versus tangent height as derived from the FWHM of each kernel (blue line).

Figure 5.4.2 shows an altitude versus latitude cross-section of CFC11 and CFC12 for 18 May 2006. All longitudes are averaged for the plots. The lifetimes of CFC11 and CFC12 in the atmosphere are relatively long (approximately 50 and 100 years respectively). Thus we may expect that the tropospheric amounts of the CFCs to be fairly uniform with the same magnitude as the surface value. Surface observations of CFCs have been made by NOAA [Elkins et al., 1994] for many years and show a slowly varying concentration with time. CFC11 surface values, from stations at latitudes from 71N to 90S, in 2006 ranged from 248 to 252 pptv; for CFC12, for the same stations and times, surface amounts were 530-540 pptv. As may be seen in Figure 5.4.2 the tropospheric amounts retrieved by HIRDLS are similar to those measured from the NOAA surface stations. There is a regularly observed excess of CFC11, of about 30%, in the upper tropical troposphere that cannot be explained at this time.

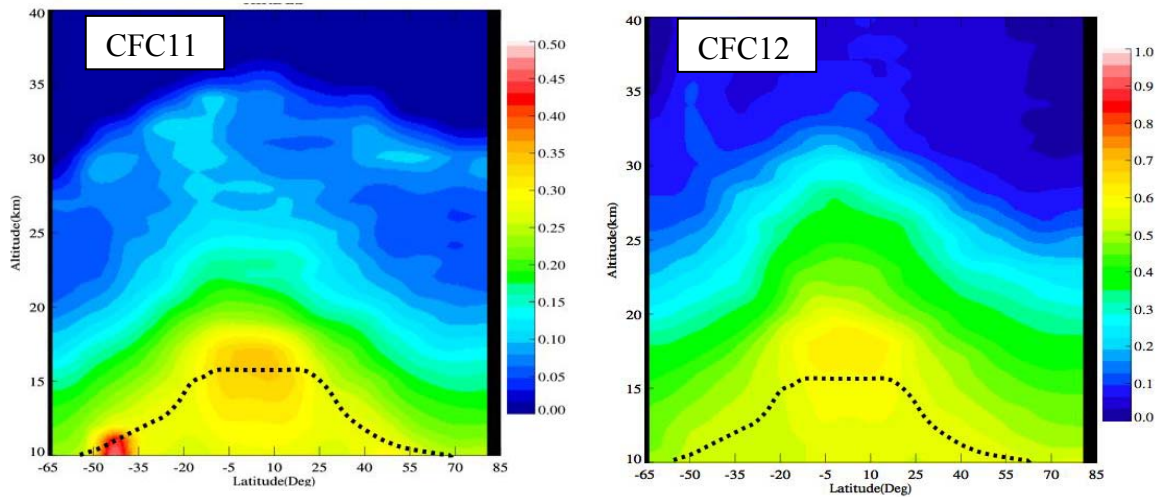


Figure 5.4.2: Latitude-altitude cross-section of CFC11 and CFC12 on 18 May 2006. Note the different color scales of the plots. The dotted line represents the approximate location of the tropopause. The high region near 45S and 10 km in the CFC11 plot is probably the effect of high cloud on the retrieval process.

Precision of the CFC measurements is composed of two main parts in the region of useful measurement, namely, error due to the retrieval process and error in the observed radiance. Figure 5.4.3 shows the precision that can be expected from the retrieval process alone. In the results of Figure 5.4.3 simulated data, with a forward model error term consisting of 0.3% of the channel radiance, are presented to the retrieval process. As may be seen in the figures the retrieval process does not limit the precision until the CFC concentration has dropped to less than half of its maximum value.

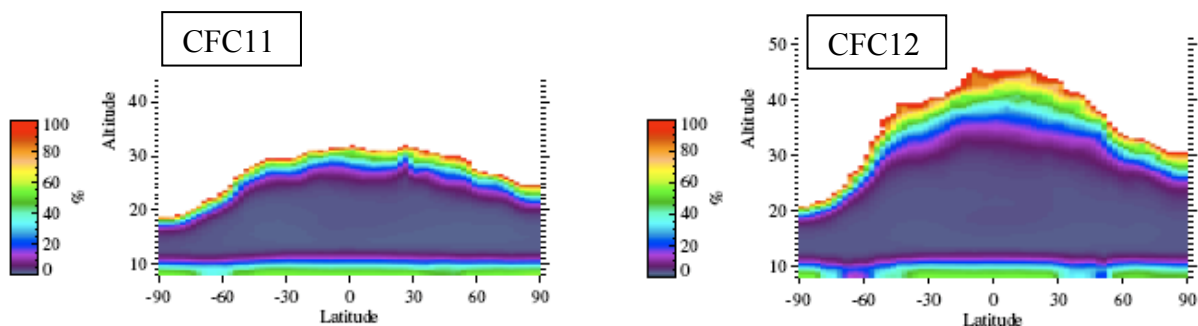


Figure 5.4.3: Precision of the retrieval process for CFC11 and CFC12. For this simulation a random error was set as 0.3 % of the channel radiance. The diagonal elements of the *a priori* covariance matrix, S_{xa}^{ii} were set at $(20 \text{ K})^2$ for temperature and $(300 \text{ \%})^2$ for species and the off-diagonal elements were calculated using a 5 km correlation length.

Due to the long lifetime of CFC11 and CFC12 a zonal average is a good representation of the vertical profile of mixing ratio at a given latitude. Figure 5.4.4 shows the zonal mean vertical profile of CFC11 and CFC12 for measurements made on 18 May 2006 between 40 and 50 N. Also shown in the figure are the standard deviations of the means and the mean precision profiles and their standard deviation. On this day the precision was generally within 30% for CFC11 and CFC12 for pressures between 200 and 6 hPa. If the variance of the total error is greater than half the variance of the *a priori* error then most of the information in a given retrieval is from the *a priori*. In those cases the precision value in the HIRDLS data archive is reported as a negative number (*CFC11Precision* and *CFC12Precision* data fields).

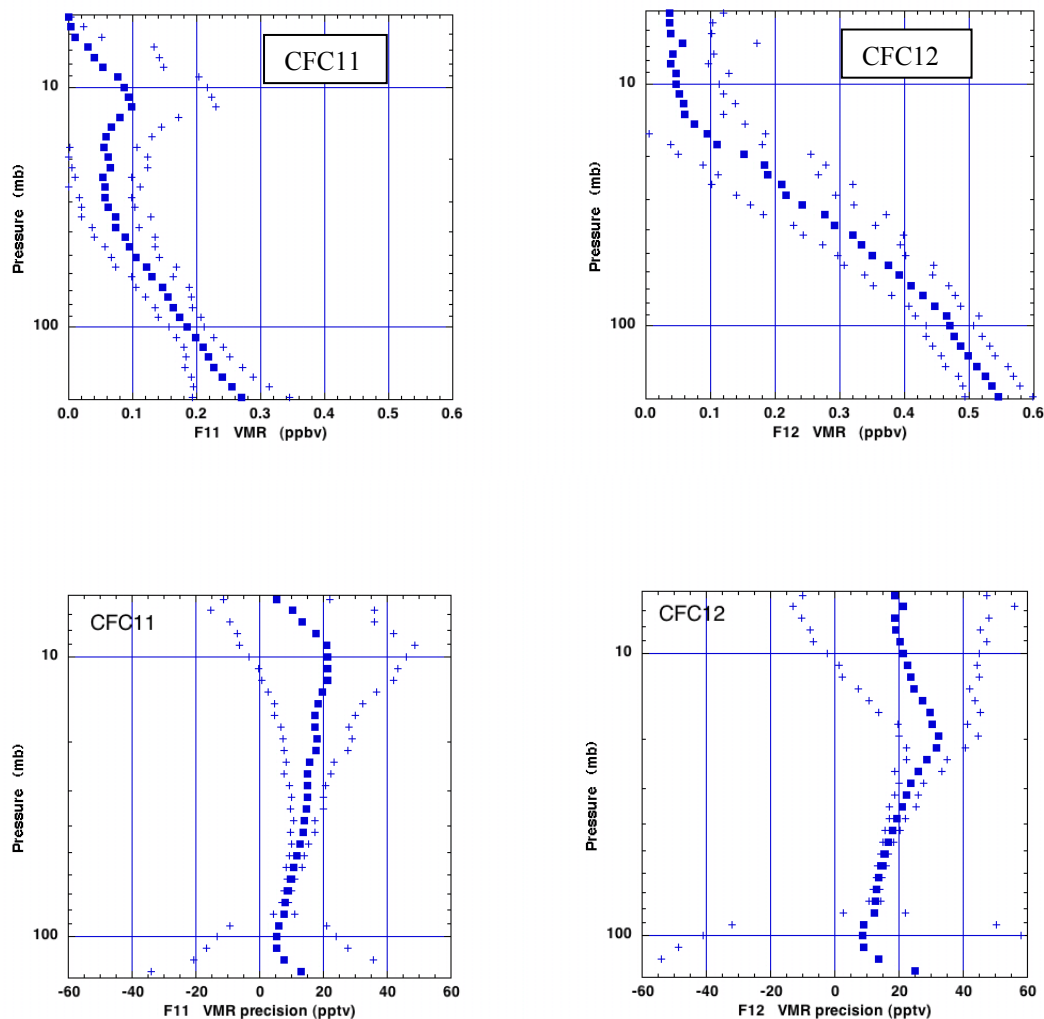


Figure 5.4.4: Zonal mean vertical mixing ratio profile for CFC11 and CFC12. Upper frames: Average for all profiles between 40 and 50 N on 18 May 2006, also showing plus and minus one standard deviation. Lower frames: Average precision in pptv and the standard deviation of the precision.

Comparisons with other measurements

Figure 5.4.5 shows the CFC11 and CFC12 vertical mixing ratio profiles from HIRDLS and results from a number of satellite and balloon-borne instruments. The satellite results are reported in Hoffmann et al, 2008, the latest results being from the space-borne MIPAS instrument on Envisat for 2002-2004. Care must be taken in comparing the older satellite observations with HIRDLS since both CFC11 and CFC12 show a clear temporal change. CFC11 surface mixing ratio increased steadily until about 1995 and has shown about a 1% per year decrease since then. The CFC12 amount, with a longer lifetime, leveled off around 1995 and is just now, in 2008, beginning to show a decrease. The plots in Figure 5.4.5 show the qualitative agreement between profiles derived by HIRDLS and those from earlier satellite experiments and from the balloon-borne JPL MkIV spectrometer. More detailed profile comparisons are shown later.

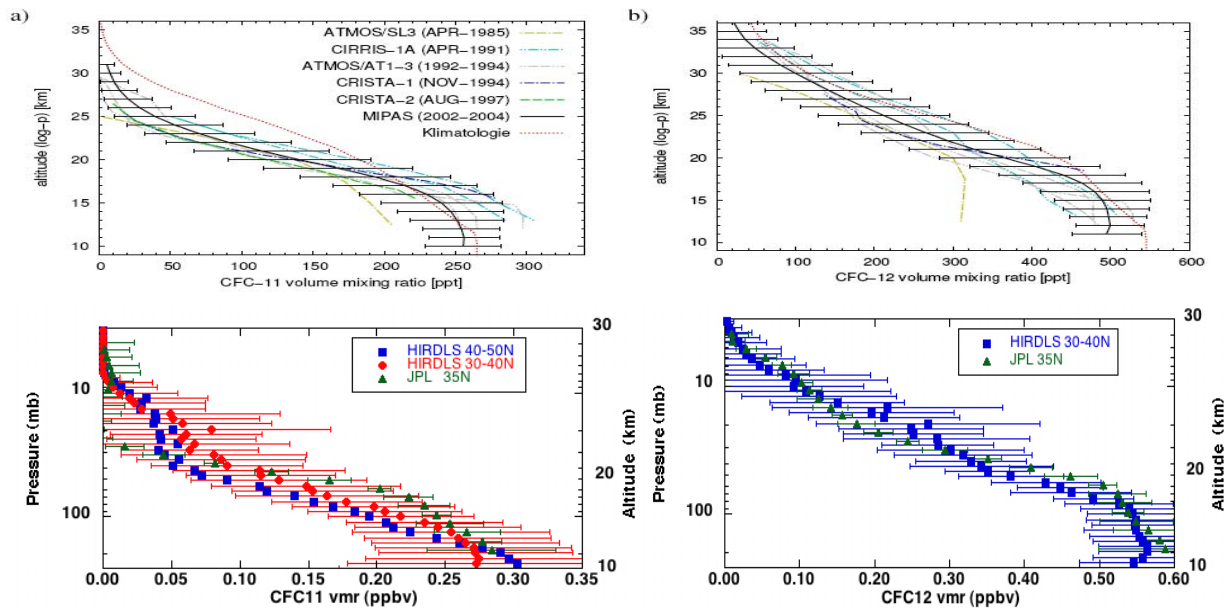


Figure 5.4.5: Vertical profiles of CFC11 and CFC12 from a number of satellite and balloon experiments (ATMOS, CIRRIS, CRISTA, MIPAS, JPL MkIV) and from HIRDLS. Observations are all from northern hemisphere mid-latitudes.

Two recent satellite-borne experiments report measurements of CFC11 and CFC12. The Michelson Interferometer for Passive Atmospheric Sounding (MIPAS) instrument aboard Envisat (launched in March, 2002) and the Atmospheric Chemistry Experiment (ACE) aboard Scisat (launched in August, 2003). Figure 5.4.6 shows altitude versus latitude plots of HIRDLS and MIPAS for one day in 2007. Reasonable agreement is seen in the CFC11 and CFC12 distributions. The high inclination (74 degree) orbit of ACE tends to concentrate coincident observations between HIRDLS and ACE in latitudes near 60 degrees (see Figure 5.3.7). Figure 5.4.7 shows all northern hemisphere HIRDLS and ACE CFC11 profiles within 2 hours and 500

km of each other and for which the measurement precision was between 0.0 and 0.3. Good agreement is found between HIRDLS and the more extensively validated ACE CFC11 observations [Mahieu et al., 2008]. No good coincidences were found between HIRDLS and ACE for CFC12.

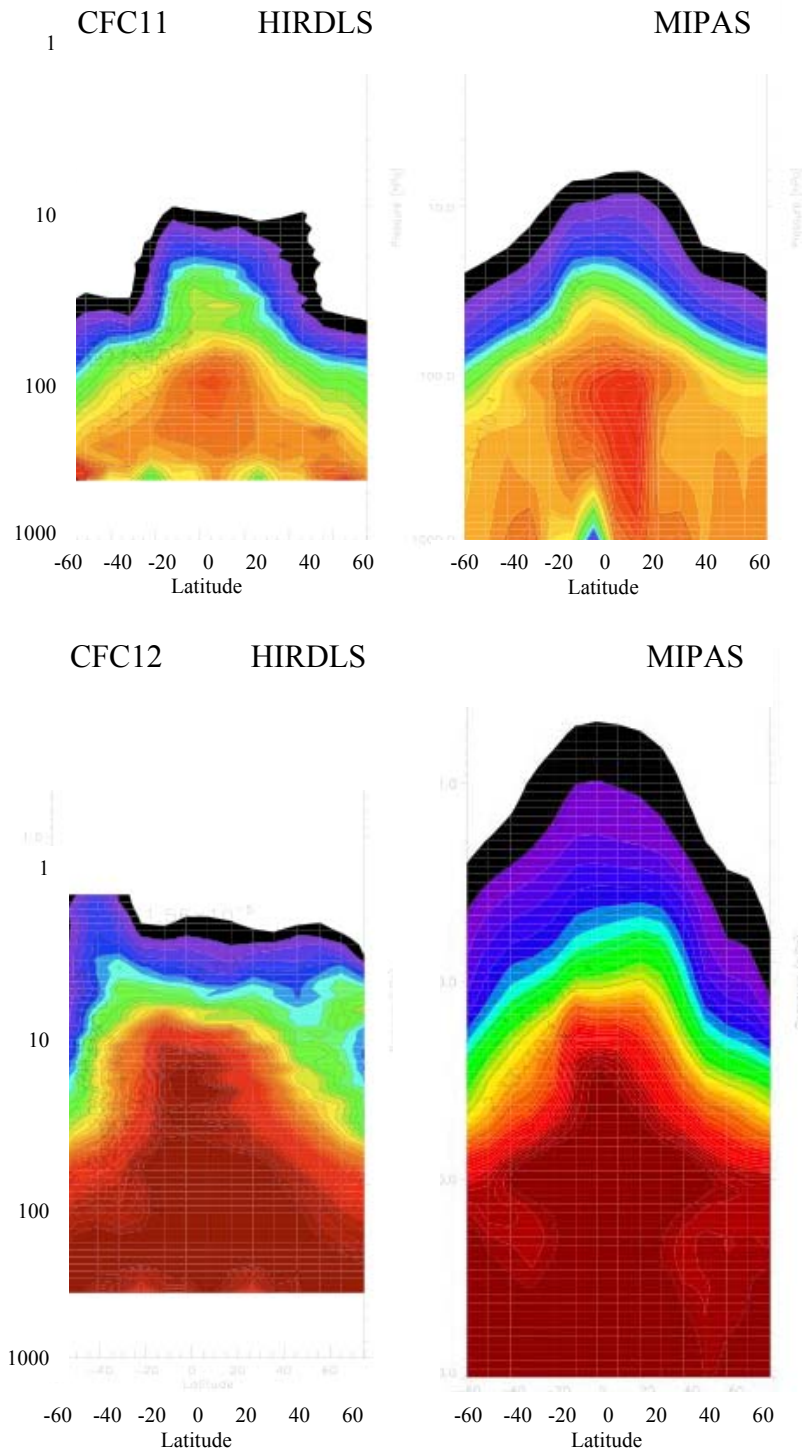


Figure 5.4.6: Altitude-latitude cross-sections of CFC11 and CFC12 as measured on the same day (2007d287) by HIRDLS and MIPAS.

CFC11 Northern Hemisphere

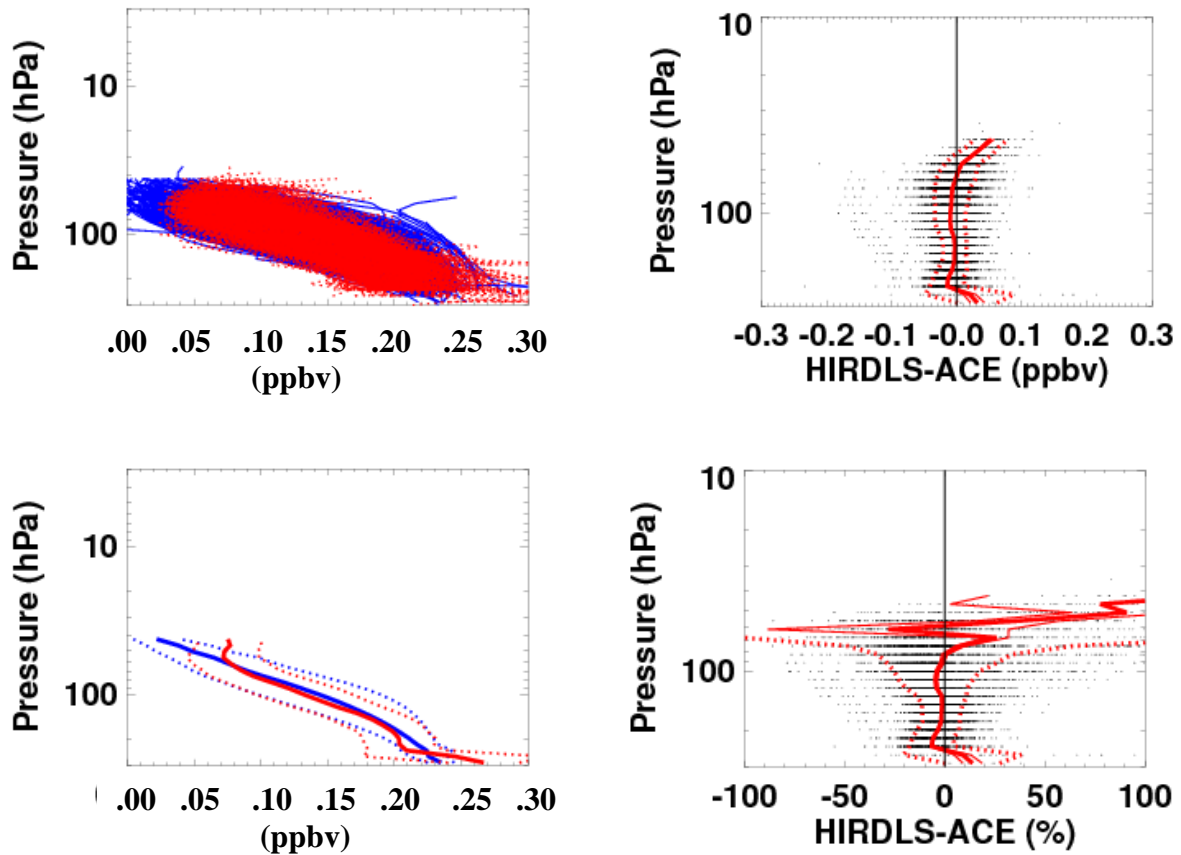


Figure 5.4.7: (Top left) Northern hemisphere profiles of CFC11 within 2 hours and 500 km and precision between 0.0 and 0.3 as measured by HIRDLS (red) and ACE (blue). (Bottom left) Average vertical profile from HIRDLS and ACE with one sigma standard deviations shown. (Top right) HIRDLS-ACE difference for coincident observations within 2 hours and 500 km. (Bottom right) Difference profile shown as a percentage of the HIRDLS observation.

CFC11 Southern Hemisphere

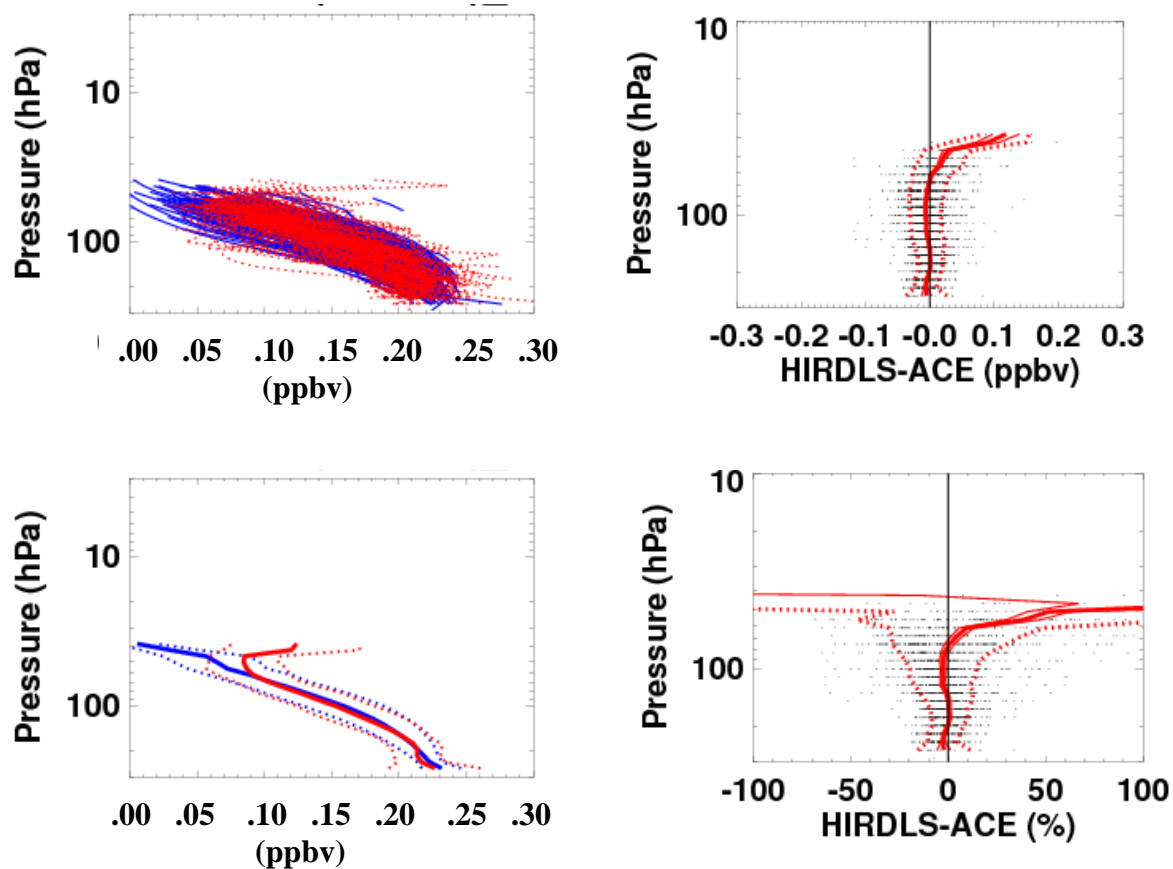


Figure 5.4.8: (Top left) Southern hemisphere profiles of CFC11 within 2 hours and 500 km and precision between 0.0 and 0.3 as measured by HIRDLS (red) and ACE (blue). (Bottom left) Average vertical profile from HIRDLS and ACE with one sigma standard deviations shown. (Top right) HIRDLS-ACE difference for coincident observations within 2 hours and 500 km. (Bottom right) Difference profile shown as a percentage of the HIRDLS observation.

References

Elkins, J.W., T.M. Thompson, J.H. Butler, R.C. Myers, A.D. Clarke, T.H. Swanson, D.J. Endres, A.M. Yashinaga, R.C. Schnell, M. Winey, B.G. Mendonca, M.V. Losleben, N.B.A. Trivett, D.E.J. Worthy, V. Hudec, V. Chorney, P.J. Fraser, and L.W. Porter. 1994. "Global and hemispheric means of CFC-11 and CFC-12 from the NOAA/CMDL flask sampling program", pp. 28-40. In T.A. Boden, D.P. Kaiser, R.J. Sepanski, and F.W. Stoss (eds.), Trends '93: A Compendium of Data on Global Change. ORNL/CDIAC-65. Carbon Dioxide Information Analysis Center, Oak Ridge National Laboratory, Oak Ridge, TN, USA.

Hoffmann, L., Kaufmann, M., Spang, R., Müller, R., Remedios, J. J., Moore, D. P., Volk, C. M., von Clarmann, T., and Riese, M.: Envisat MIPAS measurements of CFC-11: retrieval, validation, and climatology, *Atmos. Chem. Phys.*, **8**, 3671-3688, 2008.

Mahieu, E., P. Duchatelet, P. Demoulin, K. A. Walker, E. Dupuy, L. Froidevaux, C. Randall, V. Catoire, K. Strong, C. D. Boone, P. F. Bernath, J.-F. Blavier, T. Blumenstock, M. Coffey, M. De Mazière, D. Griffith, J. Hannigan, F. Hase, N. Jones, K. W. Jucks, A. Kagawa, Y. Kasai, Y. Mebarki, S. Mikuteit, R. Nassar, J. Notholt, C. P. Rinsland, C. Robert, O. Schrems, C. Senten, D. Smale, J. Taylor, C. Tétard, G. C. Toon, T. Warneke, S. W. Wood, R. Zander, and C. Servais, Validation of ACE-FTS v2.2 measurements of HCl, HF, CCl₃F and CCl₂F₂ using space-, balloon- and ground-based instrument observations, *Atmos. Chem. Phys. Discuss.*, **8**, 3431–3495, 2008.

5.5 H₂O

TBS

5.6 CH₄

TBS

5.7 NO₂

TBS

5.8 N₂O₅

TBS

5.9 ClONO₂

TBS

5.10 Cloud Products

Data	Cloud Top Pressure, Cloud Flags
Data Field Names:	CloudTopPressure, 12.1MicronCloudAerosolFlag
Useful Range:	422-10 hPa
Screening Criteria:	Some false cloud positives are present, $z > 20$ km
Vertical Resolution:	1km
Contact:	Steven Massie
Email:	massie@ucar.edu
Validation Paper	Massie <i>et al.</i> , High Resolution Dynamics Limb Sounder observations of polar stratospheric clouds and subvisible cirrus, <i>J. Geophys. Res.</i> , VOL. 112, D24S31, doi:10.1029/2007JD008788, 2007.

HIRDLS data files contain cloud flags and cloud top pressures. Details of the determination of cloud top pressures and cloud flags are discussed in Massie et al. [2007].

Cloud flag data is contained in the “12.1MicronCloudAerosolFlag” data variable. Cloud flags are stated at each pressure level when pressures correspond to altitudes between 5 and 30 km altitude. Cloud flag values are 0 (no clouds), 1 (unknown cloud type), 2 (cirrus layer), 3 (extensive Polar Stratospheric Cloud), and 4 (opaque). If the cloud flag is nonzero, then this indicates that the radiance at that pressure is measurably different from the clear sky radiance profile. Note that the total number of PSCs is equal to the number of cloud flags with values of either 1 or 4.

Comparisons of clear sky and individual radiance profiles of the various cloud types are presented in Figure 5.10.1. Note that radiance perturbations are substantial for several cloud types, since gas opacity in HIRDLS Channel 6, the 12 μm “infrared window” channel, is very low. Any cloud opacity along the HIRDLS limb-view tangent ray path produces a substantial 12 μm radiance signal.

The cloud top pressure (i.e. the ‘CloudTopPressure’ variable in the archived data file) is determined in the following manner. For a single day’s set of radiance profiles, the clear sky radiance profile for HIRDLS channel 6 is calculated by an iterative technique for several latitude bands. For the first iteration, the average profile, its standard deviation, and associated gradients from 5 to 30 km altitude, are calculated summing over all profiles. For the second iteration, profiles are tossed out of the ensemble average (based on the fact that a cloudy radiance profile deviates from the average curve). New standard deviations and associated gradients are recalculated. The iterative process continues for five iterations.

Note that the HIRDLS focal plane has three columns of detectors. The 12 μm detector is in the middle column, while the three ozone detectors 10-12 are in the first column, and the two columns are separated in distance by ~ 17 km. Situations arise in which the cloud

top structure differs along the 17 km horizontal distance, i.e. a cloud top in the first column can be higher than that in the middle column. Subsequent to the methodology and discussions in Massie et al., 2007, the cloud detection routines now also determine cloud tops in the tropics in the transparent ozone channel 12. The cloud top altitude is assigned to be the higher of the channel 12 and channel 6 cloud top altitudes.

Once the clear sky radiance profile is calculated, we determine the altitude level at which cloud radiance perturbations are first noted. The cloud top pressure (in hPa) is the pressure derived by the operational retrieval that corresponds to the cloud top altitude. Since the cloud top altitudes are on an altitude grid with one kilometer spacing, the cloud top pressure has a granularity reflective of the altitude grid spacing, e.g. for pressure level P , the cloud top pressure could be large by $\Delta P \sim P (\exp(1 \text{ km}/7 \text{ km}) - 1.0) \sim 0.15 P$.

There are some instances in which cloud flags falsely indicate the presence of clouds near and above 20 km altitude, especially at polar latitudes, outside of the seasons in which PSCs are expected to occur. These false identifications occur when radiances become very low in the 20 to 30 km altitude range.

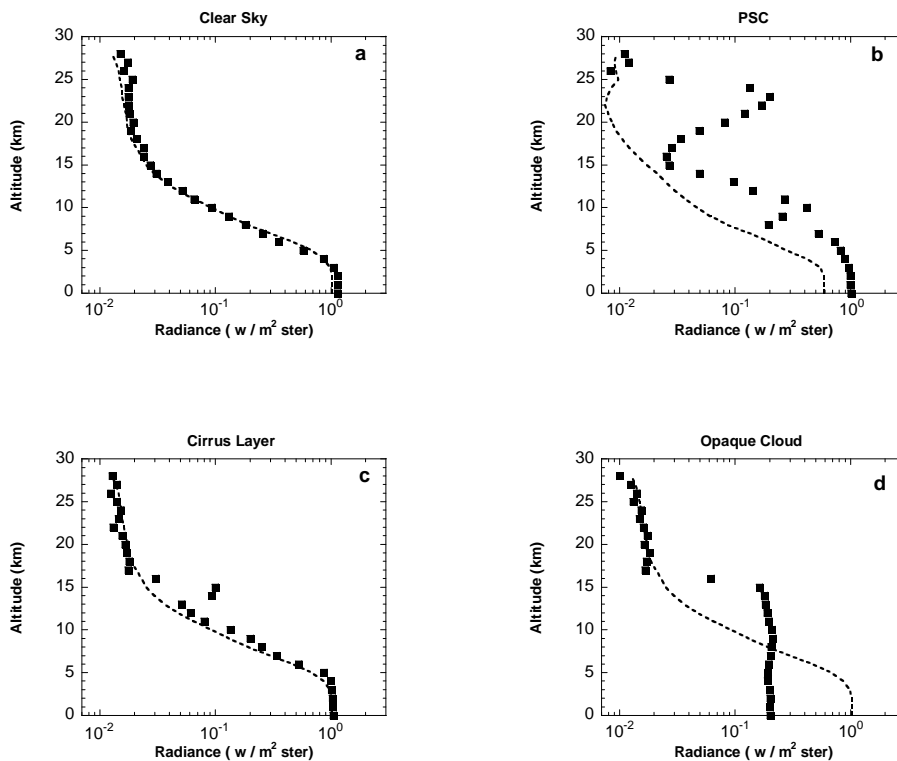


Figure 5.10.1. Four representative Channel 6 ($12.1 \mu\text{m}$) radiance (single squares) and clear sky average profiles (dotted curves) on January 27 2005, a) clear sky (15.57°N , 216.20°E), b) PSC (68.31°N , 343.41°E), c) tropical cirrus layer (4.32°N , 220.00°E), and d) opaque tropical cloud (16.79°S , 223.72°E) cases. Panels a, b, c, and d correspond to cloud flags equal to 0, 3, 2, and 4, respectively.

HALOE and HIRDLS time averaged cloud top pressures have correlation coefficients of 0.66 and 0.92 in the tropics and mid-latitudes, respectively (see Figure 5.10.2). Massie et al. 2007 cite correlations of 0.87 and 0.93 in the tropics and mid-latitudes for HIRDLS cloud top data in 2005 and HALOE data from 1998 to 2005. The inclusion of the channel 12 ozone cloud top determination to the cloud detection process in the tropics has changed the cloud top statistics from the previous determination.

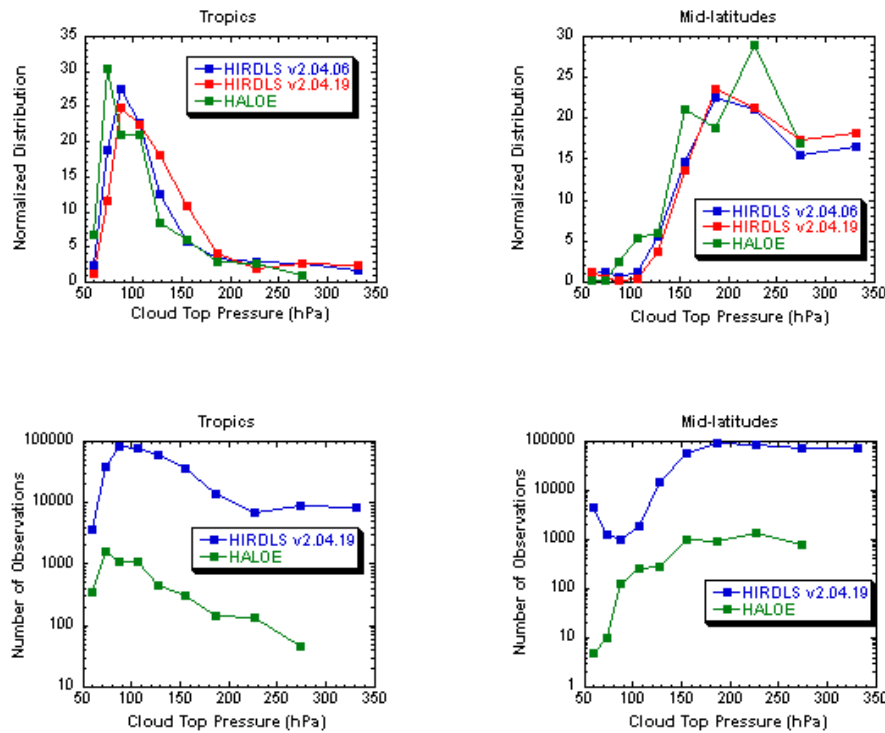


Figure 5.10.2 A comparison of HIRDLS and HALOE cloud top pressures statistics for the previous (v2.04.06) and current (v2.04.19) data versions for data in 2005 and 2006, respectively, and HALOE data from 1998 through 2005.

Since the standard gas species retrievals terminate at the cloud top, the frequency of retrieval of gas species will decrease as pressures increase. The fraction of the time for which clouds are absent along HIRDLS limb paths in 2007 is presented in Figure 5.10.3. The latitudinal variation of the cloud free percent frequency is primarily influenced by the location of the tropopause. While the cloud free percent frequency is low at higher pressures, the number of cloud free profiles is still large at higher pressures due to the large number of profiles (~5500 per day) measured by the HIRDLS experiment.

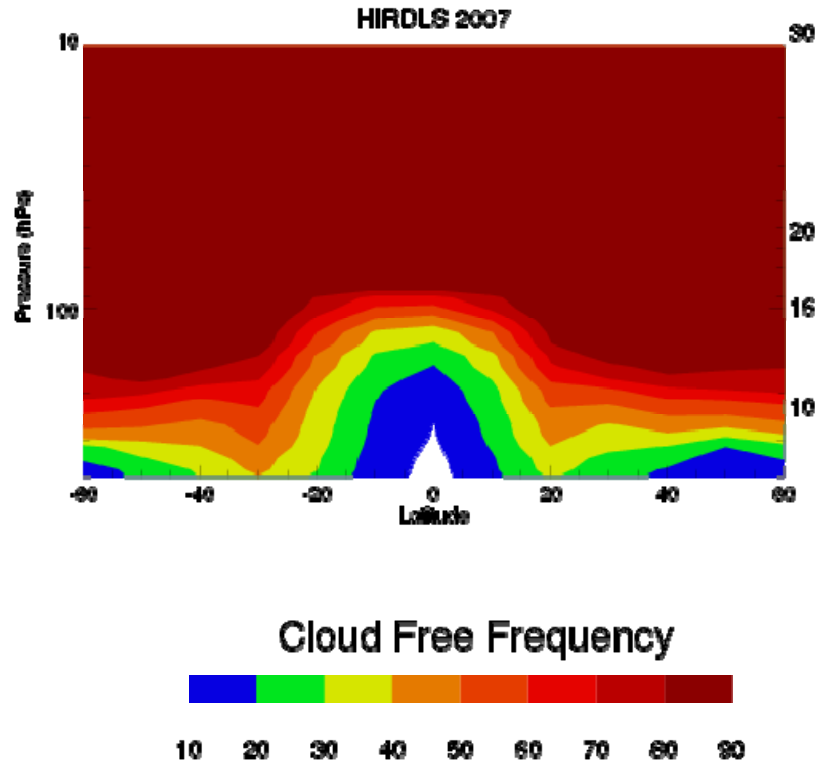


Figure 5.10.3. Cloud-free frequency in 2007. All pressures below the cloud top pressure of a single radiance profile are considered to be influenced by clouds. An approximate altitude scale in kilometers is given on the right hand side of the figure.

Data	12.1 Micron Extinction
Data Field Name:	12.1MicronExtinction
Useful Range:	215-20 hPa
Screening Criteria	Use extinction in a qualitative manner Use extinction between 10^{-5} to 10^{-2} km^{-1} Precision/data in 0 to 100% range
Vertical Resolution:	1km
Contact:	Steven Massie
Email:	massie@ucar.edu

Cloud and aerosol extinction and extinction precisions, in units of km^{-1} , at $12\ \mu\text{m}$ are included in the “12.1MicronExtinction” and “12.1MicronExtinctionPrecision” data fields. The recommended range of pressure for the extinction is 20 to 215 hPa. Data above and below this range of pressure is flagged as -999 in the current data version. It is recommended that extinction in the range of 10^{-5} to 10^{-2} km^{-1} be used when the precision is positive from 0 to 100%. Two week (or longer) zonal (hPa versus latitude) averages of extinction above the tropopause are recommended for the sulfate aerosol extinction in the stratosphere.

The 20 hPa pressure limit was determined from comparisons of HIRDLS extinction profiles with correlative profiles. HIRDLS extinction profiles at pressure levels less than 20 hPa increased in value, which is unrealistic. The higher pressure range of extinction was selected due to the fall off of extinction retrieval frequency, which is less than 80% and 50% in the mid-latitudes and tropics, respectively, at pressures greater than 215 hPa. Geospatial patterns of cloud extinction in latitude-longitude maps were very coherent at pressures from 215 hPa up to the tropopause. Future releases of extinction will hopefully be extended to pressures greater than 215 hPa.

Since the 12 μm channel radiances are very low (which makes this “infrared window” especially good for detecting clouds), the absolute calibration of the radiances is still problematic. The extinction for the retrieved sulfate aerosol is larger than correlative measurements (i.e. HALOE extinction zonal averages and University of Denver size distributions, converted to extinction profiles via Mie calculations) by a factor of ~ 2 . For this reason the data should be used in a qualitative manner, whereby the extinction data is used to indicate sulfate (low) extinction versus cloud extinction in a relative manner. Cloud extinction at 12 μm is present when the extinction is greater than approximately $9 \times 10^{-4} \text{ km}^{-1}$ (i.e. the cloud extinction threshold determined previously by John Mergenthaler based upon analyses of the 12 μm extinctions of the CLAES experiment on the UARS platform).

Figure 5.10.4 presents latitude-longitude graphs of HIRDLS extinction for January 2006 at several pressure levels near the tropopause. The extinction averages are similar to those obtained by previous solar occultation experiments, with maxima over the maritime continent, Africa, and South America. Figure 5.10.5 presents seasonal graphs of extinction for winter and summer at 121 hPa to illustrate seasonal variations in cloud extinction. Monsoon dynamics influence the distribution of clouds over India during summer, while deep convection during winter produces high cloud frequencies over the maritime continent.

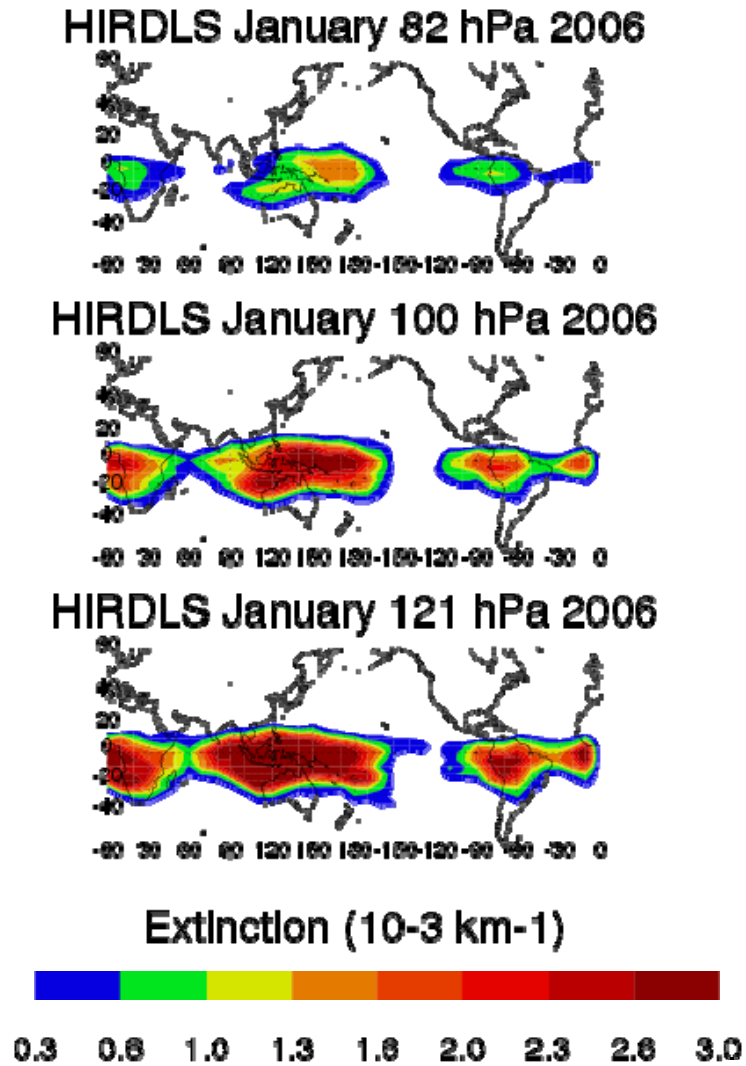


Figure 5.10.4. HIRDLS extinction for January 2006 at several pressure levels near the tropopause.

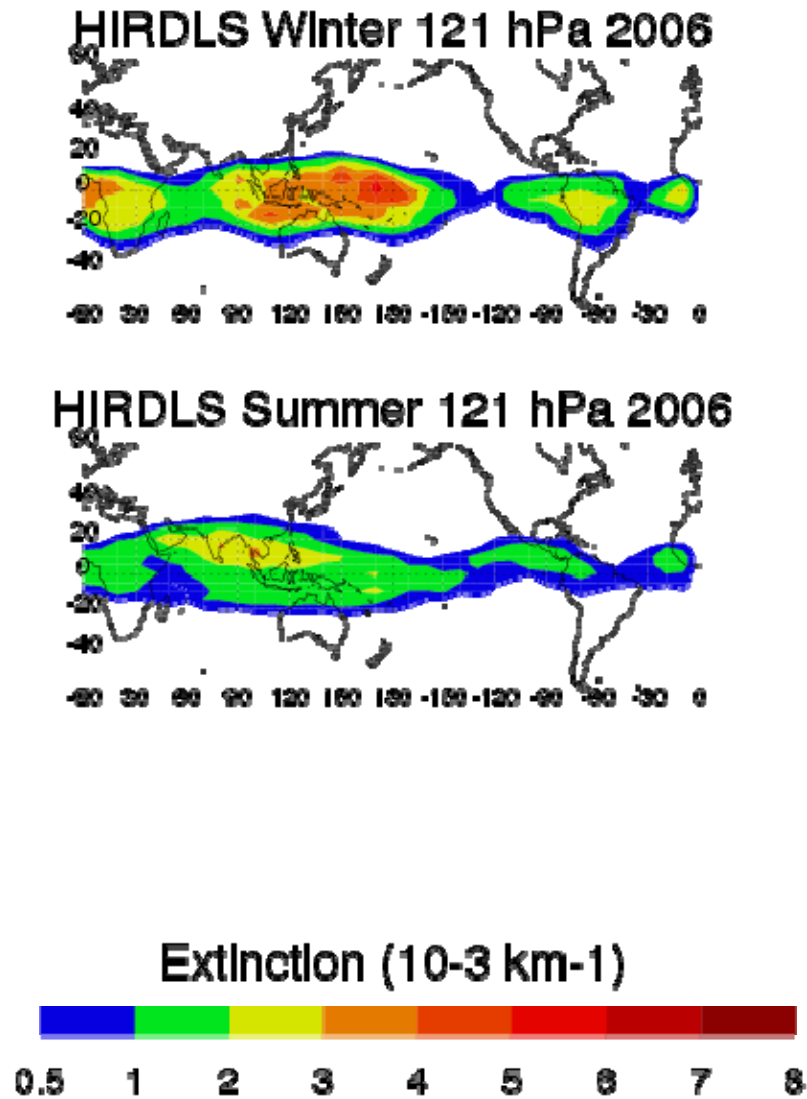


Figure 5.10.5. Winter and summer HIRDLS extinction at 121 hPa during 2006.

Reference: Massie, S. T. et al., HIRDLS Observations of PSCs and Subvisible Cirrus, 2007: J. Geophys. Res., doi:10.1029/2007JD008788.

6.0 Data File Structure and Content

Contact: Cheryl Craig
Email: cacraig@ucar.edu

HIRDLS Level 2 data are stored in the HDF-EOS5 format and the fields are as described in the [_HDF-EOS Aura File Format Guidelines_ document](#)¹. These data files can be read via C/C++ or Fortran using either the HDF-EOS5 or HDF5 library. HIRDLS has developed both an IDL routine "get_aura" and a set of Fortran90 routines to access the HIRDLS Level 2 data. Both of these routines are available for download via the HIRDLS web site, <http://www.eos.ucar.edu/hirdls/data/access.shtml>. The routines can also be supplied via email upon request.

Users should obtain the pre-compiled HDF5 library for their operating system, if possible, otherwise source code is also available (see <http://hdf.ncsa.uiuc.edu>). These are prerequisite in order to compile the HDF-EOS5 library (see <http://www.hdfeos.org/>). Both libraries are needed to fully access the Aura HIRDLS data files. For additional help contact the GES DISC at help-disc@listserv.gsfc.nasa.gov or telephone 301-614-5224.

Each HIRDLS Level 2 file contains one day's worth of data and contains all species that HIRDLS measures. A number of the fields are filled completely with missing values until correction algorithms are refined for these species. For users who require only a subset of the HIRDLS species, the Goddard DISC has the ability to subset data before distributing it to users. Contact the DISC directly for more information on this service.

Individual HIRDLS data values for a product are stored in fields labeled with the species name (see the appropriate section above for the exact Data Field Name). The estimated precision of each data point is a corresponding field named *SpeciesPrecision* (for instance, Temperature and TemperaturePrecision). Two additional fields for each species, *SpeciesNormChiSq* and *SpeciesQuality*, are both filled with missing for V004. CloudTopPressure does not have Precision, NormChiSq or Quality fields.

There are two time fields in the HIRDLS data file, *Time* and *SecondsInDay*. *Time* is stored in TAI time (seconds since the epoch of UTC 12 AM 1-1-1993). This time includes leap seconds and can cause problems with simplistic conversions. For this reason, HIRDLS is also storing *SecondsInDay* which is seconds since midnight of the data day. Leap seconds do not pose a problem when using this field. Note that the first data point may be negative which indicates a time stamp before midnight. This is the case for scans which span a day boundary.

¹http://www.eos.ucar.edu/hirdls/HDFEOS_Aura_File_Format_Guidelines.pdf

7.0 Algorithm Changes

<u>HIRDLS Version</u>	<u>DISC Version</u>	<u>Changes</u>
2.00	001	[Baseline]
2.01		Modified to process Scan Table 22
2.02.07	002	Modified to process Scan Tables 30, 13, 22 and 23
2.04.09	003	Modified to include more precise geo-location, updated cloud detection, updated calibration constants, and bug fixes.
2.04.19	004	Added new products: CFC11, CFC12, 12.1 micron aerosol extinction. Implemented updated open area fractions, improved cloud detection and out-of-field correction. Added correction for instrument-spacecraft alignment (equivalent to 2 Km shift).

8.0 Acronyms

ACE	Atmospheric Chemistry Experiment
ACD-FTS	Atmospheric Chemistry Experiment Fourier Transform Spectrometer
ATBD	Algorithm Theoretical Basis Document
ATMOS	Atmospheric Trace Molecule Spectroscopy
CFC	Chlorofluorocarbons
CIRRIS	Cryogenic Infrared Radiance Instrumentation for Shuttle
CRISTA	Cryogenic Infrared Spectrometers and Telescopes for the Atmosphere
DISC	Data and Information Services Center
ECMWF	European Center for Medium range Weather Forecasting
EOS	Earth Observing System
FWHM	Full Width Half Maximum
GES DISC	Goddard Earth Sciences Data and Information Services Center
GMAO	Goddard Modeling and Assimilation Office
HALOE	Halogen Occultation Experiment
HDF5	Hierarchical Data Format Version 5
HDF-EOS5	HDF for EOS Version 5
HIRDLS	High Resolution Dynamics Limb Sounder
HIRDLS1C	High Resolution Dynamics Limb Sounder Level 1 Data
IDL	Interactive Data Language
JPL	Jet Propulsion Laboratory

L0	Level 0
L0-1	Level 0-1
L1	Level 1
L1-2	Level 1-2
L1C	Level 1 Corrector
L1PP	Level 1 Pre-processor
L1X	Level 1 Excellerator
L2	Level 2
L2CLD	Level 2 Cloud Detector
L2PP	Level 2 Pre-processor
LHS	Left Hand Side
LOS	Line Of Sight
MIPAS	Michelson Interferometer for Passive Atmospheric Sounding
MkIV	Mark IV Spectrometer
MLO	Mauna Loa Observatory
MLS	Microwave Limb Sounder
NASA	National Aeronautics and Space Administration
NCAR	National Center for Atmospheric Research
NH	Northern Hemisphere
NOAA	National Oceanic and Atmospheric Administration
OMI	Ozone Monitoring Instrument
OLR	Outgoing Longwave Radiation
PIs	Principal Investigators
PSC's	Polar Stratospheric Clouds
PV	Pressure Volume
RHS	Right Hand Side
RMS	Root Mean Square
SAGE III	Stratospheric Aerosol and Gas Experiment III
S/C	Spacecraft
s.d.	Standard Deviation
SHADOZ	Southern Hemisphere ADditional OZonesondes
ST	Scan Table
TAI	International Atomic Time
TES	Tropospheric Emission Spectrometer
TMF	Table Mountain Facility
UK	United Kingdom
USA	United States of America
UTC	Coordinated Universal Time
UTLS	Upper Troposphere – Lower Stratosphere
V003	Version 3

V004	Version 4
VMR	Volume Mixing Ratio
WAVES	Water Vapor Validation Experiment Satellite/Sondes
WOUDC	World Ozone and Ultra-Violet Radiation Data Center